ACS OMEGA

http://pubs.acs.org/journal/acsodf

Review

Stochastic Nature and Intramolecular Coupling in Optical Response Profiles: Critical Analysis through Semiclassical Models

José Luis Paz,* Marcos A. Loroño, Lenin A. González-Paz, Edgar Márquez, José R. Mora, and Ysaias J. Alvarado

Cite This: *ACS Omega* 2023, 8, 10690−10712

Read Online

ACCESS | Metrics & More | Article Recommendations

ABSTRACT: We have studied the nonlinear absorptive and dispersive responses considering a molecular system consisting of two-levels, where aspects of the vibrational internal structure and intramolecular coupling are inserted, in addition to the considerations of interaction with the thermal reservoir. The Born−Oppenheimer electronic energy curve for this molecular model consists of two-intercrossing harmonic oscillator potentials with minima displaced in energy and nuclear coordinate. The results obtained show how these optical responses are sensitive to explicit considerations of both intramolecular coupling and the presence of the solvent through their stochastic interaction. Our study shows that the permanent dipoles of the system and the transition dipoles induced by electromagnetic field effects represent critical quantities for the analysis. The solvent action in our model is treated through the natural Bohr frequency shift to a time-dependent function, with explicit manifestations in its comparison as if the upper state were broadened. Significant variations in the nonlinear optical properties for cases of perturbative and saturative treatments, relaxation times, and optical propagation, mainly due to changes in the probe and pump intensities, are studied. Our studies relating the intramolecular effects with those generated by the presence of the solvent and its stochastic interaction with the solute of study, have allowed not only to analyze the influence of these in the profile of the optical responses, but they could also provide some insights into the analysis and characterization of molecular systems through nonlinear optical properties.

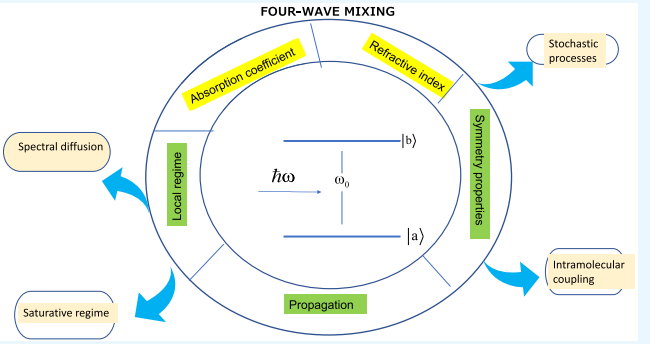

1. INTRODUCTION

The present work explores the sensitivity of the nonlinear optical responses of molecular systems, selected as models, associated with organic dyes, and subjected to different considerations in the radiation−matter interaction process. We use a widely studied multiphotonic Four-Wave mixing (FWM) process as an interaction scheme.[1] Many authors[2−7] have performed theoretical studies of the nonlinear optical responses of different quantum systems to compare these results with the nonlinear responses experimentally found in organic molecules.[8] Using two-state systems a nonlinear optical response of organic dye molecules, such as Malachite Chloride Green (MCG) and Cyanine dye (Diethyl Quinolylthia-iodinated Carboxycyanide), also known as DQCI, has been described. The organic dye MCG has also been described by three quantum state systems,[4] being that the theoretical study of Nonlinear Optical properties NLO of quantum systems developed mainly through polarization spectroscopy[7] and four-wave mixing FWM spectroscopy.[8] Mourou,[6] measured the hole burning width in a band of the 0−0 transition in cryptocyanine in methanol through an inhomogeneously broadened two-state model and a four-state model at which two of its states were broadened. Yajima et al.[8] studied ultrafast relaxation times in electronic transitions of DQCI in ethanol. Song et al.[4] explained dichroism and birefringence in DQCI and MCG molecules through NLO. Souma et al.[9] studied the dissipation mechanisms and relaxation times in Rhodamine B and DQCI in ethanol. Garcia-Golding[5] presented a theoretical model and with the support of experimental data estimated the product of MCG and DQCI relaxation times and studied the saturation effects of the pumping beam on the population decay of this dye in different solvents.[3] With the purpose of limiting the present work of revision referring to the NLO, our considerations will be referred to classic descriptions of the electromagnetic field and varied situations of the chemical system of study with emphasis in

Received: November 14, 2022
Accepted: March 1, 2023
Published: March 16, 2023

detailing the molecular structure and how this one, can have influences of correlation in the description of the NLO.[10−16] Al-Saidi and Abdulkareen[17] pointed out important modifications in the optical properties in chemical solutions as a function of the concentration of the organic dye being analyzed, the variation being a direct effect from a nonlinear saturable absorption, as an important issue in the analysis of optical limiters. The effect of propagation in pulsed FWM, of spontaneous or counter propagating nature, and the theory derived from the propagation effects in this nonlinear time-resolved process, puts into perspective the relevance of knowing the behavior of the beams in their optical path, where the absorptive and dispersive processes play an important role in understanding the propagation, as well as in deciphering some properties associated with symmetry, inherent to the incident and emerging fields in the FWM scheme.[18]

A more exhaustive review of the recent literature shows a very high interest in four-wave mixing spectroscopy both in its fundamental conception and in its various applications, which include the study of multiphotonic processes, as well as those of technological development, characterization of materials, optical communications, optomechanics, coherent control, optical trapping, tweezers, among others.[19−28] It should also be noted that, as part of the extensive application of this technique and its varied model formulation, the use of characterization tools through nonlinear optical properties highlighting more explicit considerations of solvent action, quantum effects, and functionalized organic compounds, have been the subject of recent work by many authors.[29−32]

We present a scheme, which involves both a molecular system and different approaches to describe the interaction with an incident electromagnetic field. Unlike many other works already presented in literature, our work incorporates fundamental relevance in the FWM process. On the source of the fluctuations, different modifications of the longitudinal relaxation times T_1 and transversal relaxation times T_2 occur.[1,33] Both the longitudinal relaxation time and the transverse relaxation time are associated with all those relaxation-dissipation processes present in the interaction between matter and electromagnetic fields. Thus, for all those situations where the solute strongly interacts with the thermal reservoir, stochastic modeling is the most convenient if one wishes to describe the randomness in the set of solute−solvent collisions.[34] Here, molecular collisions can induce a shift of the deterministic Bohr frequency, and due to their collisional nature, generate a stochastic modulation in the transition frequency. In cases where the mechanism associated with the relaxation process is modified at the originally deterministic transition frequency associated with the molecular system, and this frequency follows a radiation−matter interaction, then the dynamic equations associated with the Bloch vector would be of the integro-differential type, making the OCBEs no longer fully valid in the description.[35] It is known from the literature that a two-state system model to describe the molecular system is of great utility in nonlinear optics and even in quantum optics. Normally such states are associated with the vibrational part associated with one or two potential energy surfaces of the molecule under study. For many years an attempt has been made to provide a sound physical explanation for the description of the new vibrational progressions emerging because of the Herzberg−Teller vibronic coupling in absorption spectra and quantum beams.[36] Given the complexity of the model that simultaneously considers molecular structure through vibronic coupling and frequency shift due to solvent involvement, in this paper we will present the most relevant aspects of both effects. This work exhibits different models about the molecular structure of the chemical solute exposed to radiation and in the presence of the solvent, all within a framework of density matrix calculations, the OCBE and Optical Stochastic Bloch equations (OSBE), the polarizations induced in the medium and finally, the temporal and spatial electrodynamic dynamics that account for the intensity of the emerging FWM field, as well as the optical responses of the system under study. We will present different calculation schemes, based on cumulant theories and use of convolution theorems. We will emphasize the propagation processes of electromagnetic fields along the optical length for the study of tunable parametric amplifications with organic dyes and their experimental correspondence proposed by Yajima[37] and Souma et al.[9]

2. THEORY

2.1. Simple Molecule Model. Several studies have been presented in the nonlinear optics literature where the subsystem of study contemplates a simple molecule description, considering a two-level scheme.[38] Developments presented by Mollow,[39] Boyd et al.,[40] Agarwal and Nayak,[41,42] Paz et al.,[43] Boyd and Sargent,[44] Gruneisen et al.,[45] among others, for the description of the matter−radiation interaction. Paz et al.[46] and Franco et al.[47] studied in FWM signals the symmetry properties in a frequency space constituted by the detuning of the optical beams involved. Considering two incident electromagnetic fields of optical frequencies ω_1 and ω_2 resonant with a transition $|a\rangle \rightarrow |b\rangle$, the temporal evolution of the system in the formalism of the density matrix, associated with the OCBE, is given by

$$\frac{d\rho_{ba}}{dt} = -\frac{i}{\hbar}H_{ba}\rho_D - (1/T_2 + i\omega_0)\rho_{ba} = \frac{d\rho_{ab}^*}{dt} \tag{1a}$$

$$\frac{d\rho_D}{dt} = -\frac{2i}{\hbar}(H_{ab}\rho_{ba} - \rho_{ab}H_{ba}) - \frac{1}{T_1}(\rho_D - \rho_D^{(0)}) \tag{1b}$$

with $\rho_D \equiv \rho_{aa} - \rho_{bb}$. The radiative interaction $H_{ba} = -[\vec{\mu}_{ba}\cdot\vec{E}_1\cdot e^{-i\omega_1 t} + \vec{\mu}_{ba}\cdot\vec{E}_2\cdot e^{-i\omega_2 t}] + cc$; the superscript (0) denotes the equilibrium value; $\vec{\mu}_{ba}$ is the nondiagonal transition moment; $\vec{E}_1$ and $\vec{E}_2$ are the electric-field amplitudes of the pump and probe, respectively. In these equations, longitudinal T_1 and transversal T_2 relaxation times are assumed as phenomenological parameters, introduced to represent relaxations of the population and of the optically induced dipole, respectively. The solution at steady state for $\rho_{ba}(2\omega_1 - \omega_2)$ at third order in the total field, is given by

$$\rho_{ba}(\omega_3) = -\frac{2i}{\hbar}\left[\frac{(\vec{\mu}_{ba}\cdot\vec{E}_1)^2(\vec{\mu}_{ba}\cdot\vec{E}_2^*)}{\Gamma_1(\Delta)D_3}\right]\left(\frac{1}{D_1} + \frac{1}{D_2^*}\right)\rho_D^{(0)} \tag{2a}$$

where $\Gamma_1(\Delta) = \frac{1}{T_1} - i\Delta$, $D_j = \frac{1}{T_2} + i(\omega_0 - \omega_j)$ for $j = 1, 2, 3$ and $\Delta = \omega_1 - \omega_2$. The FWM intensity is proportional to $|\vec{P}|^2$, with $\vec{P} = N\langle\rho_{ba}\cdot\vec{\mu}_{ab}\rangle$, defined as the nonlinear macroscopic polarization; N is the chemical concentration, $\langle\cdots\rangle_\theta$ denotes an ensemble average over the initially isotropic orientational distribution. The intensity $I(\Delta_1,\Delta)$ of this FWM signal, is given by

https://doi.org/10.1021/acsomega.2c07300
ACS Omega 2023, 8, 10690−10712

$$I(\Delta_1, \Delta) = \left[I_{max}\left(\Delta^2 + \frac{4}{T_2^2}\right)\right] / \left[3T_1^2T_2^4\left(\frac{1}{T_1^2} + \Delta^2\right)\left(\frac{1}{T_2^2} + \Delta_1^2\right)\left(\frac{1}{T_2^2} + (\Delta_1 - \Delta)^2\right)\left(\frac{1}{T_2^2} + (\Delta_1 + \Delta)^2\right)\right] \quad (2b)$$

with $I_{max} = I(0,0)$ and $\Delta_j = \omega_j - \omega_0$ and where is valid $I(\Delta_1, \Delta) = I(-\Delta_1, -\Delta)$, $I(\Delta_1, \Delta) = I(-\Delta, \Delta_1)$ and $I(\Delta_1, \Delta) = I(\Delta, -\Delta)$, are the inherent symmetry properties of eq 2b, independent of the sign of Δ and Δ_1. However, the FWM response is asymmetric with respect to the transformation $\Delta_2 \rightarrow -\Delta_2$ analyze the resonant FWM spectrum for the cases of homogeneous and inhomogeneous broadening lines.[47] Differences in the forms of the spectra, such an asymmetry, saturation and AC Stark splitting, can be used to discriminate whether the spectrum is homogeneously or inhomogeneously broadened. Reif et al.[48] study the optical propagation in homogeneous lines, highlighting the possibility of analysis under three regimes differentiated by pump intensity. Marquez et al.[49] study the saturation effects and dynamic Stark effects on the FWM signal in the frequency space. Paz et al.[50] defines the characteristics of a resonant FWM signal in the frequency space. Paz et al.[51] study the properties of the resonance peaks associated with the nondegenerate FWM signal in a system with defined permanent dipole moments. Topological properties and the dominant contributions of the coherence and/or population that determine the intensity and spectral line width, are studied.

2.1.1. Induces Coherence Studies and Inhomogeneous Macroscopic Nonlinear Polarization. Several studies have been carried out using FWM to measure ultrashort relaxation times characteristic of molecular systems, particularly of organic compounds.[52] Studies using FWM techniques, including the Stark effect, and applied to the understanding of the instabilities occurring in electromagnetic fields through absorption media.[44] Introducing a perturbation expansion for the density, we obtain the following steady-state relationships in the RWA for the coherence at frequency ω_m:

$$\rho_{ba}(\omega_m) = i\frac{\tilde{\rho}_D^{dc}}{D_m}\{\Omega_m + J[\Omega_1\delta_{m,3} + \Omega_2\delta_{m,1}] + J^*[\Omega_1\delta_{m,2} + \Omega_3\delta_{m,1}]\} \quad (3)$$

with m = 1, 2, 3 for the pump, probe, and FWM signal, respectively, and where J is given by

$$J = \frac{2}{|G_2|^2}\{-\tilde{\Omega}_1\tilde{\Omega}_2^*G_1 - \tilde{\Omega}_3\tilde{\Omega}_1^*G_2\lambda_{3,-1} + \tilde{\Omega}_1\tilde{\Omega}_3^*G_3\} \quad (3a)$$

$$G_1 = \left[\frac{1}{T_1} + i\Delta_{12}\right] + 2|\Omega_1|^2\lambda_{1,-2}\lambda_{2,-3}$$

$$G_2 = \left[\frac{1}{T_1} + i\Delta_{12}\right] + 2|\Omega_1|^2\lambda_{2,-3} + 2|\Omega_2|^2(D_1^*)^{-1}$$

$$G_3 = 2|\Omega_2|^2\lambda_{1,-1}\lambda_{1,-3}$$

$$\lambda_{n,-m} = \left[\frac{2}{T_2} + i\Delta_{nm}\right](D_nD_m^*)^{-1}$$

$$D_{2n+1} = \frac{1}{T_2} + i[\omega_0 - (\omega_1 + n\Delta_{12})]$$

with the notation $n = 0, -1, 1$ for pump, probe, and FWM signal, respectively, and considering $D_{-1} \equiv D_2$, for $\Delta_{nm} = \omega_n - \omega_m$. The zero frequency Fourier component is given by $\rho_D^{dc} = \rho_D^{(0)}\Phi$ where the Φ function is given by

$$\Phi = [(1 - q) + 4S(T_2^2|D_1|^2)^{-1}]^{-1}; \quad S = |\Omega_1|^2T_1T_2 \quad (3b)$$

Here, we have defined S is the saturation parameter associated with the pump beam. The q-function is given by

$$q = 4T_1[|\Omega_1|^2|\Omega_2|^2(\lambda_{1,-2}\lambda_{1,-2}(G_2^*)^{-1} + \lambda_{2,-1}\lambda_{2,-1}(G_2)^{-1}) + (\Omega_1^*)^2\Omega_2\Omega_3(\lambda_{2,-1}(G_2D_1)^{-1} + \lambda_{3,-1}\lambda_{1,-2}(G_2)^{-1})] \quad (3c)$$

The Rabi frequency is defined as $\Omega_k = \vec{d}_{BA}\cdot\vec{E}(\omega_k)/\hbar$ for k = 1, 2, 3. From eq 3 we have $\rho_{ba}(\omega_1)$, $\rho_{ba}(\omega_2)$, and$\rho_{ba}(\omega_3)$, as Fourier components of the coherences associated with the three beams, and where it is possible to derive:

$$\rho_{ba}(\omega_1) = \beta_1\Omega_1 + \varepsilon_1\Omega_2(\Omega_3\Omega_1^*) \quad (4a)$$

$$\rho_{ba}(\omega_2) = \beta_2\Omega_2 + \varepsilon_2\Omega_1(\Omega_1\Omega_3^*) \quad (4b)$$

$$\rho_{ba}(\omega_3) = \beta_3\Omega_3 + \varepsilon_3\Omega_1(\Omega_1\Omega_2^*) \quad (4c)$$

β_j considers the coherent and incoherent contributions in the absorption and scattering processes, while ε_j refers to the coupling processes that take place between the beams.

https://doi.org/10.1021/acsomega.2c07300
ACS Omega 2023, 8, 10690−10712

$$\beta_1 = i\frac{\rho_D^{dc}}{D_1} - 2i\frac{|\Omega_2|^2\rho_D^{dc}\lambda_{1,-2}}{D_1}$$

$$\beta_2 = i\frac{\rho_D^{dc}}{D_2} - 2i\frac{|\Omega_1|^2\rho_D^{dc}\lambda_{2,-1}}{D_2 J^*}$$

$$\beta_3 = i\frac{\rho_D^{dc}}{D_3} - \left[2i\frac{|\Omega_1|^2\lambda_{3,-1}}{D_3 J} - 4i\frac{|\Omega_1|^2|\Omega_2|^2\lambda_{1,-1}\kappa_{2,-1}}{D_3 J J^*}\right]\rho_D^{dc}$$

$$\varepsilon_1 = -\frac{2i}{D_1}\left(\frac{\lambda_{3,-1}}{J} + \frac{\lambda_{2,-1}}{J^*}\right)\rho_D^{dc}$$

$$\varepsilon_2 = -\left(\frac{2i\lambda_{1,-3}}{D_2 J^*} - \frac{4i\,|\Omega_2|^2\lambda_{1,-1}\lambda_{1,-2}}{D_1 J J^*}\right)\rho_D^{dc}$$

$$\varepsilon_3 = -\frac{2i\lambda_{1,-2}}{D_3 J}\rho_D^{dc}$$

$$J = \frac{1}{T_2} - i\Delta_{12} + 2\,|\Omega_1|^2\lambda_{3,-2} + \frac{2\,|\Omega_2|^2}{D_1}$$

We can notice in the expressions of β_j and ε_j that there are only explicit dependencies with the amplitudes of the fields, but no dependence on either the optical length (z) or with respect to time. For the evaluation of the polarization components, an integration is performed on the inhomogeneous distribution of the resonance frequencies of the two-level systems $|a\rangle$, $|b\rangle$, given by

$$\vec{P}(\omega_j) = N\int_{-\infty}^{\infty} d\omega_0 L(\omega_0)\langle\rho_{ba}(\omega_j)\vec{d}_{ab}\rangle_\theta \tag{5}$$

N represents the number of active molecules per unit volume, $L(\omega_0)$ is the Lorentzian distribution describing the inhomogeneous spectral line of the response for the two-state system ensemble. The bracket over θ, reflects an average over the vector orientations of both the fields and the induced moments, and $L(\omega_0)$ is given by

$$L(\omega_0) = \frac{1}{\pi}\left(\frac{\gamma}{(\omega_0 - \omega_c)^2 + \gamma^2}\right) \tag{6}$$

γ represents the half-width at the half-height (HWHM) and ω_c is the center of the Lorentzian distribution. The integration calculation is solved by employing the complex variable techniques and using the residue theorem, for a closed contour selection in the upper half-plane:

$$P(\omega_1) = \chi_{eff}^{incoh}(\omega_1, z)E(\omega_1) + \chi^{SV}(\omega_1)E(\omega_1) \tag{7a}$$

$$P(\omega_2) = [\chi_{eff}^{incoh}(\omega_2, z) + \chi_{eff}^{coh}(\omega_2, z)]E(\omega_2) + \chi_{eff}^{coup}(\omega_2, z)E(\omega_1)E(\omega_1)E^*(-\omega_3) + \chi^{SV}(\omega_2)E(\omega_2) \tag{7b}$$

$$P(\omega_3) = [\chi_{eff}^{incoh}(\omega_3, z) + \chi_{eff}^{coh}(\omega_3, z)]E(\omega_3) + \chi_{eff}^{coup}(\omega_3, z)E(\omega_1)E(\omega_1)E^*(-\omega_2) + \chi^{SV}(\omega_3)E(\omega_3) \tag{7c}$$

$\chi^{SV}(\omega_k)$ with $(k = 1, 2, 3)$represents the electrical susceptibility for the solvent at frequency ω_k. This susceptibility is not derived from the calculation, it only refers to the presence of the solvent; $\chi_{eff}^{coh}(\omega_k z)$ and $\chi_{eff}^{incoh}(\omega_k z)$represent the effective components of the electrical susceptibilities that account for the coherent and incoherent contributions to the absorption and scattering of the weak beams; $\chi_{eff}^{coup}(\omega_k z)$ represents the effective components of the electrical susceptibility that refers to the coupling process between the pumping beam with the pumping-signal and pump−probe oscillation networks, for the generation of photons at the probe and signal frequencies, respectively.

$$\chi_{eff}^{incoh}(\omega_1, z) = -AT_2\left\{\frac{1 + \gamma T_2 - i(\omega_c - \omega_1)T_2}{A_0} + \frac{1 + \tilde{T}_2\sqrt{\tilde{S}}}{B_0}\right\} \tag{8a}$$

$$\chi_{eff}^{incoh}(\omega_k, z) = -A\left\{\frac{[1 + T_2^2(\omega_c - \omega_1 + i\gamma)][1 + \gamma T_2 - iT_2(\omega_c - (\omega_1 + n\Delta_{12}))]}{A_1^{\pm}} - \frac{4S[1 + T_2\sqrt{\tilde{S}} \pm i\Delta_{12}T_2]}{B_1^{\pm}} + \frac{2 \pm \Delta_{12}T_2[2i \pm \Delta_{12}T_2]}{C_1^{\pm}}\right\} \tag{8b}$$

$$\chi_{eff}^{coup}(\omega_k, z) = \frac{2Ad_{AB}^2T_2^2}{\hbar^2}\left\{\frac{[1 + \gamma T_2 - iT_2(\omega_c - \omega_1)]}{A_2^{\pm}} + \frac{1 + T_2\sqrt{\tilde{S}}}{B_2^{\pm}} + \frac{1 - iT_2(\pm a + bi)}{F_2^{\pm}}\right\} \times \frac{\left[\frac{2}{T_2} \pm (-i\Delta_{12})\right]}{[\Gamma\delta_{k,3} + \Gamma^*\delta_{k,2}]} \tag{8c}$$

$$\chi_{eff}^{coh}(\omega_k, z) = \frac{2A}{T_1T_2}\left\{\{[[1 - \gamma T_2 + iT_2(\omega_c - \omega_1)][1 + \gamma T_2 - iT_2(\omega_c - \omega_2)][1 + \gamma T_2 - iT_2(\omega_c - \omega_3)]]/[A_3^{\pm}]\} + \frac{[1 - T_2\sqrt{\tilde{S}}][(1 + T_2\sqrt{\tilde{S}})^2 + \Delta_{12}^2T_2^2]}{B_3^{\pm}} + \frac{(\pm 4i\Delta_{12}T_2)[1 - (\pm)i\Delta_{12}T_2]}{C_3^{\pm}} + \frac{[1 + iT_2(\pm a + bi)][(1 - iT_2(\pm a + bi))^2 + \Delta_{12}^2T_2^2]}{F_3^{\pm}}\right\} \frac{\left[\frac{2}{T_2} \pm (-i\Delta_{12})\right]}{[\Gamma\delta_{k,3} + \Gamma^*\delta_{k,2}]}S \tag{8d}$$

valid $k = 2, 3$ and where $A = \frac{2N\gamma d_{ab}^2\rho_D^{(0)}}{\hbar T_2^3}$; $\tilde{S} = \frac{1 + 4S}{T_2^2}$; $\Gamma = \frac{1}{T_1} - i\Delta_{12}$. The coefficients have been defined as

https://doi.org/10.1021/acsomega.2c07300
ACS Omega 2023, 8, 10690−10712

$$A_0 = 2i\gamma[(\omega_c - \omega_1 + i\gamma)^2 + \tilde{S}]$$

$$B_0 = 2i[(\omega_1 - \omega_c + i\sqrt{\tilde{S}})^2 + \gamma^2]\tilde{S}$$

$$A_1^{\pm} = A_0\left[(\omega_c - (\omega_1 + n\Delta_{12}) + i\gamma)^2 + \frac{1}{\tilde{T}_2^2}\right]$$

$$B_1^{\pm} = B_0\left[(\pm\Delta_{12} + i\sqrt{\tilde{S}})^2 + \frac{1}{T_2^2}\right]$$

$$C_1^{\pm} = \frac{2i}{T_2}\left[\left(\omega_1 + n\Delta_{12} - \omega_c + \frac{i}{T_2}\right)^2 + \gamma^2\right]\left[\left(\pm\Delta_{12} + \frac{i}{T_2}\right)^2 + \tilde{S}\right]$$

$$A_2^{\pm} = A_0[(\omega_c - \omega_1 + i\gamma)^2 - (\pm a + ib)^2]$$

$$B_2^{\pm} = -B_0[(\pm a + bi)^2 + \tilde{S}]$$

$$F_2^{\pm} = 2[(\omega_1 - \omega_c \pm a + bi)^2 + \gamma^2][\tilde{S} + (\pm a + bi)^2](\pm a + bi)$$

$$A_3^{\pm} = A_2^{\pm}\left[(\omega_c - (\omega_1 + n\Delta_{12}) + i\gamma)^2 + \frac{1}{T_2^2}\right]$$

$$B_3^{\pm} = B_2^{\pm}\left[(\mp\Delta_{12} + i\sqrt{\tilde{S}})^2 + \frac{1}{T_2^2}\right]$$

$$C_3^{\pm} = C_1^{\pm}\left[\left(\pm\Delta_{12} + \frac{i}{T_2}\right)^2 - (\pm a + bi)^2\right]$$

$$F_3^{\pm} = F_2^{\pm}\left[(\pm\Delta_{12} \pm a + bi)^2 + \frac{1}{T_2^2}\right]$$

we have defined $a + bi = \sqrt{\omega_1^2 - \omega_q^2}$

$$\omega_q^2 = \omega_{qR}^2 + i\omega_{qI}^2 = \left(\omega_2\omega_3 + \frac{1}{T_2^2} + \frac{4S(1 + T_1T_2\Delta_{12}^2)}{T_2^2(1 + T_1^2\Delta_{12}^2)}\right) + i\left(\frac{2\Delta_{12}}{T_2}\right)\left(\frac{4S(T_1 - T_2)}{T_2(1 + T_1^2\Delta_{12}^2} - 1\right)$$

Therefore:

$$a = -\frac{\omega_{qI}^2}{2b}$$

$$b = \frac{1}{\sqrt{2}}\sqrt{\omega_{qR}^2 - \omega_1^2 + \sqrt{(\omega_{qR}^2 - \omega_1^2)^2 + (\omega_{qI}^2)^2}}$$

$(n, k, \pm)$ correspond to $(1, 3, +)$ for the signal field, while $(-1, 2, -1)$ for the probe field. It is important to note the characteristics and symmetries in the terms of eq 7a. The coherent term associated with the pumping beam does not appear, as well as the coupling term between the considered beams.

2.1.2. Optical Propagation Studies. Considering the Fourier components of the inhomogeneous macroscopic polarization for each electromagnetic field, we have calculated through Maxwell's equation, how the electric field intensity is modified with respect to the optical propagation length (z), considering the effects of the molecular structure linked to the intramolecular coupling. We consider the scalar approximation and the slowly envelope approximation,[1] and we have in a general form:

$$\frac{d\tilde{E}_1}{dz} + \tilde{\alpha}_1(\omega_1, z)\tilde{E}_1 = \Psi_1^{(2,3)}(\omega_1, z)\tilde{E}_1^* \exp(i\Delta k_z z) \quad (9a)$$

$$\frac{d\tilde{E}_2}{dz} + \tilde{\alpha}_2(\omega_2, z)\tilde{E}_2 = \Psi_2^{(1,1)}(\omega_2, z)\tilde{E}_3^* \exp(i\Delta k_z z) \quad (9b)$$

$$\frac{d\tilde{E}_3}{dz} + \tilde{\alpha}_3(\omega_3, z)\tilde{E}_3 = \Psi_3^{(1,1)}(\omega_3, z)\tilde{E}_2^* \exp(i\Delta k_z z) \quad (9c)$$

where $\tilde{E}_j = (E_{0j}/2)\exp(i\vartheta_j)$(electromagnetic fields envelope); ϑ_j is the phase angle and finally, $\tilde{\alpha}_j\ (\omega_j, z)$ is the nonlinear absorption coefficient for a frequency ω_j. In our case:

$$\tilde{\alpha}_j(\omega_j, z) = \frac{2\pi\omega_j}{\eta_j c} Im(\chi_{\text{eff}}^{\text{coh}}(\omega_j) + \chi_{\text{eff}}^{\text{incoh}}(\omega_j)) \quad j = 2, 3 \quad (10)$$

and in the case of the pump beam:

$$\tilde{\alpha}_1(\omega_1, z) = \frac{2\pi\omega_1}{\tilde{\eta}_1 c} Im(\chi_{\text{eff}}^{\text{incoh}}) \quad (11)$$

and where $\tilde{\eta}_j(\omega_j, z)$ is the refraction index given by[53]

$$\tilde{\eta}_j(\omega_j, z) = [1 + 4\pi Re(\chi^{\text{SV}}(\omega_j) + \chi_{\text{eff}}^{\text{coh}}(\omega_j) + \chi_{\text{eff}}^{\text{incoh}}(\omega_j))]^{1/2} \quad j = 2, 3 \quad (12)$$

and

$$\tilde{\eta}_1(\omega_1, z) = [\eta_0^2 + 4\pi Re(\chi_{\text{eff}}^{\text{incoh}}(\omega_1))]^{1/2} \quad (13)$$

for pump-beam.

The incoherent component of the susceptibility accounts for the reduction of the population difference due to the presence of saturating pumping. The coherent part involves an interference process between the weak and strong beams and arises from the presence of a population oscillation at the Δ_{12} detuning frequency. Here, $\Psi_k^{(p,q)}(\omega_k, z)$ are defined as the coupling parameters, given by

$$\Psi_k^{(p,q)}(\omega_k, z) = \frac{2\pi i\omega_k}{\tilde{\eta}_k c}\chi_{\text{eff}}^{\text{coup}}(\omega_k, z)\tilde{E}_p(\omega_p, z)\tilde{E}_q(\omega_q, z) \quad (14)$$

$\Delta k_z \approx 2k_{1z} - (k_{2z} + k_{3z})$, is the z-component of the vector mismatch, which can be written as $\Delta k_z \approx \frac{\omega}{c}(2\tilde{\eta}_1 - (\tilde{\eta}_1 + \tilde{\eta}_3)\cos\theta)$, where θ is the angle between $\vec{k}_1$ and $\vec{k}_2$. We have considered that $\Psi_1^{(2,3)}(\omega_1, z) \approx 0$ for the perturbative treatment in the probe (first order). It is necessary to point out that both $\tilde{\alpha}_1(\omega_1, z)$ and $\Psi_k^{(p,q)}(\omega_k, z)$ have a z-dependence that comes exclusively from the z-dependence of the pump beam, given its intensity variation with the optical path. That is, $\tilde{\alpha}_j\ (\omega_j, z) = \tilde{\alpha}_j(\omega_j, S(z))$ and $\Psi_k^{(p,q)}(\omega_k, z) = \Psi_k^{(p,q)}(\omega_k, S(z))$. Eq 9a can be written as follows:

$$dS/dz = -2\alpha_1 S \text{ with } S = |\tilde{\Omega}_1|^2 T_1\tilde{T}_2 \quad (15a)$$

Using eqs 11 and 8a, we obtain

https://doi.org/10.1021/acsomega.2c07300
ACS Omega 2023, 8, 10690−10712

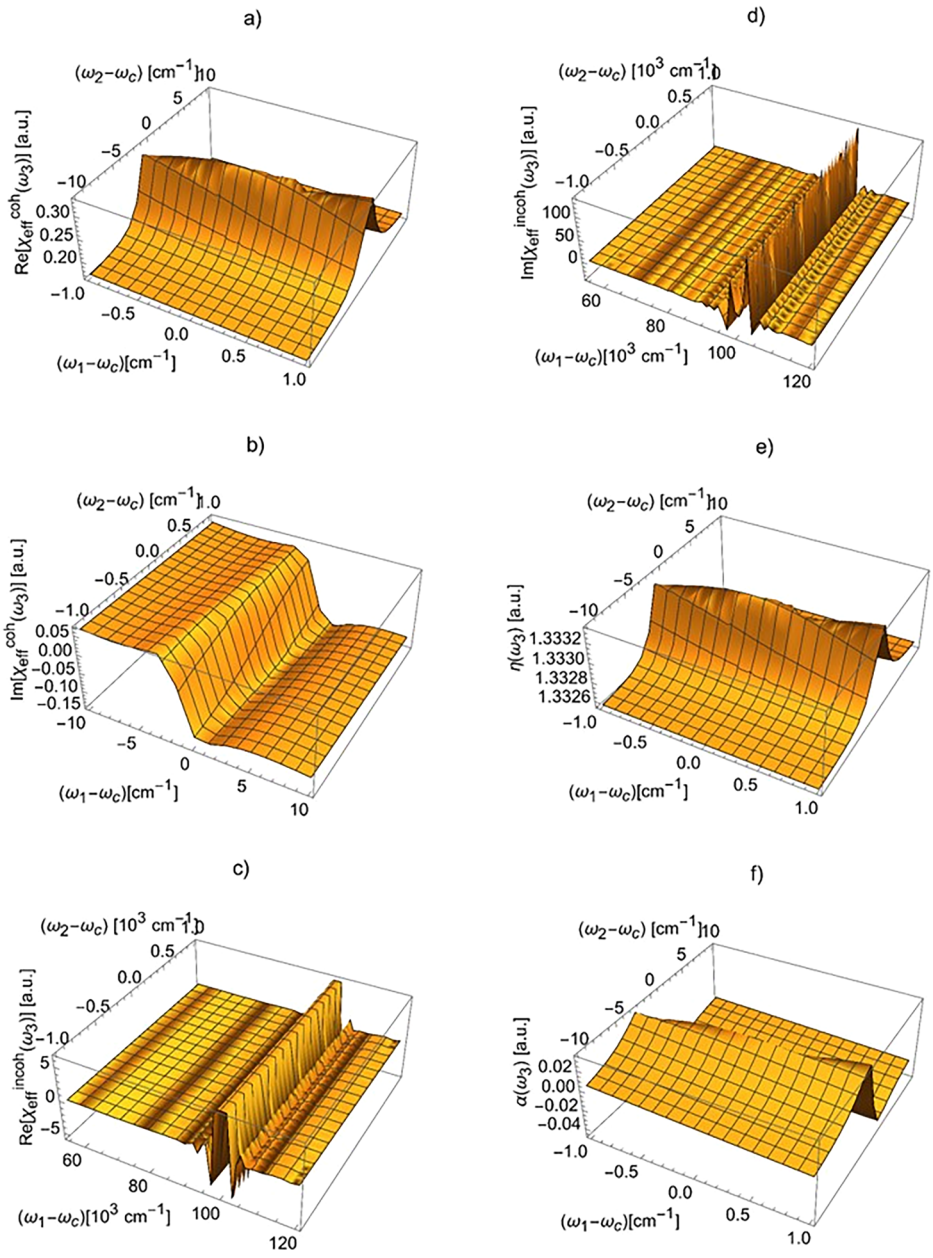

Figure 1. Susceptibility components and optical properties with frequency ω_3, as a function of the detuning of the pumping beam $(\omega_1 - \omega_c)$ and detuning of the probe beam $(\omega_2 - \omega_c)$ under the conditions $N = 0.5 \times 10^{-3}$ M, $z = 10^{-4}$ cm, and $\gamma = 10^{-4}T_2$: (a) real part of the coherent effective susceptibility, (b) imaginary part of the coherent effective susceptibility, (c) real part of the incoherent effective susceptibility, (d) imaginary part of the incoherent effective susceptibility, (e) dispersive property, and (f) absorptive property.

$$\frac{dS}{dz} = -\frac{N\pi {d_{ab}}^2 \omega_1 T_2 \rho_D^{(0)} \sum_{m=0}^{5} p_m Y^m}{\hbar c \eta_1 \sum_{m=0}^{2} q_m Y^{2m+1}} \text{ with } Y = T_2\sqrt{\tilde{S}} \tag{15b}$$

where the coefficients p_m and q_m are given by $p_0 = -\gamma T_2\Delta_+$; $p_1 = \Delta_-$; $p_2 = \gamma T_2(\Delta_+ + 1)$; $p_3 = -(\Delta_- + 1)$; $p_4 = -\gamma T_2$; $p_5 = 1$; $q_0 = \Delta_+^2$; $q_1 = -2\Delta_-$; $q_2 = 1$; with $\Delta_\pm = T_2{}^2(\gamma^2 \pm (\omega_c - \omega_1)^2)$ as a measure of the effective (dimensionless) inhomogeneous line width. This allows us to decouple eqs 9b and 9c and express the FWM signal as

$$\frac{d^2\tilde{E}_3}{dz^2} + h_1(z)\frac{d\tilde{E}_3}{dz} + h_2(z)\tilde{E}_3 = 0 \tag{16}$$

where $h_1(z)$ and $h_2(z)$ are given by

$$h_1(z) = \alpha_2 + \alpha_3 - \frac{d \ln \Psi_3^{(1,1)}}{dS}\left(\frac{dS}{dz}\right) - i\Delta k_z - iz\frac{d\Delta k_z}{dS}\left(\frac{dS}{dz}\right) \tag{16a}$$

$$h_2(z) = \alpha_2\alpha_3 - \Psi_2^{(1,1)}\Psi_3^{(1,1)} + \frac{d\alpha_3}{dS}\left(\frac{dS}{dz}\right) - \alpha_3\left[\frac{d \ln \Psi_3^{(1,1)}}{dS}\left(\frac{dS}{dz}\right) + i\Delta k_z + iz\frac{d\Delta k_z}{dS}\left(\frac{dS}{dz}\right)\right] \tag{16b}$$

Note that the explicit knowledge of the amplitude of the FWM signal requires the variations in z of the functions $h_1(Z)$ and

https://doi.org/10.1021/acsomega.2c07300
ACS Omega 2023, 8, 10690−10712

$h_2(Z)$, dependent in turn on α_j, $\Psi_j^{(p,q)}$, Δk_z, and their variations in the derivative. Here we will analyze the case where there is a variation z through the derivative in z of $S(z)$. It is possible to demonstrate their solution regimes for $S(z)$ depending on the initial value of the pump-intensity: (a) $4S(0) \ll 1$ therefore $S(z) = S(0)\exp(-2\alpha_1 z/a)$, (b) $4S(0) \gg 1$, therefore $S(z) = S(0) - \alpha_1 z/2a$, with $a = 1 + (\omega_0 - \omega_1)^2 T_2^2$, and finally for the case (c) $4S(0) \approx 1$, where $S(z)\exp(4S(z)) = S(0)\exp(4S(0)/a)\exp(-2\alpha_1 z/a)$ is a transcendent solution. To study the absorptive and dispersive characteristics of FWM signal, we used surfaces in a frequency space. In those plots, we have represented the refractive index, the absorption coefficient, and the real and imaginary parts of the coherent and incoherent nonlinear susceptibility, all of them, as a function of the detuning frequencies of both incident fields. We have set the relaxation times as $T_1 = 10T_2$ and $T_2 = 1$ ps. The resonance frequency is centered at $\omega_0 = 3.1 \times 10^{15}$ rad/s with an inhomogeneous line width $\gamma = 10^{-4} T_2^{-1}$, which corresponds to organic dye solutions such as MCG. The optical length $z = 10^{-4}$ cm and an initial intensity of pump $S(z = 0) = 2$, which is an appropriate value to observe high order effects in the intensity of the nonlinear signal and to invalidate the approximation of a constant pump-field.[46] Figure 1a shows the real part of the optical coherent susceptibility in the frequency space at the concentration and length conditions shown. It shows a typical refractive profile centered on the solvent index. We observe, the negative value of its imaginary parts shows characteristics of a negative absorption along the $\omega_1 - \omega_c$ line in frequency space (Figure 1b) (imaginary part of the coherent susceptibility). Regions of positive absorptions are attributed to strong dephasing between the dipolar response and the response of the populations under analysis.

An oscillatory behavior is detected around $\omega_1 - \omega_c = 100$ cm^{-1}, for both, its real and imaginary parts associated with the incoherent optical susceptibilities (Figure 1c, 1d). Figures e and f show the refractive and absorptive profiles in relation to their real and imaginary parts, respectively, both in the frequency space associated with the frequency detuning of the incident beams. The incoherent contribution to absorptive and dispersive responses is attributed to the reduction in the population differences due to the saturation caused by the pumping beam. The coherent nonlinear susceptibility is the principal contribution, which dictates the shape of the surfaces of the refractive index and the absorption coefficient. Finally, we have observed that when considering the propagation in this detuning space, the symmetry associated with the local regimes tends to be broken, invariantly at low or high pump intensity. The combined effects of inhomogeneous width decrease in chemical concentration and the value of the saturation parameters at the beginning of the optical path, conditional on the T_1/T_2 ratio decrease the asymmetry.

2.2. Spectral Diffusion. *2.2.1. Two-State Quantum System Incorporating Spectral Diffusion and a Reservoir State.* In this quantum model it is considered that the frequency distribution of two-state systems is described by a Lorentzian curve, so that both the base state and the excited state correspond to bands; it is considered that there is internal relaxation, i.e., there are transitions within the bands of the base state and the excited state.

The scheme is shown in Figure 2, where relaxations up to the reservoir state are observed S_{2S}^R. Mourou[6] and Garcia-Golding[5] considered that there is a natural frequency distribution; in their work, they attributed the nature of the frequency distribution to

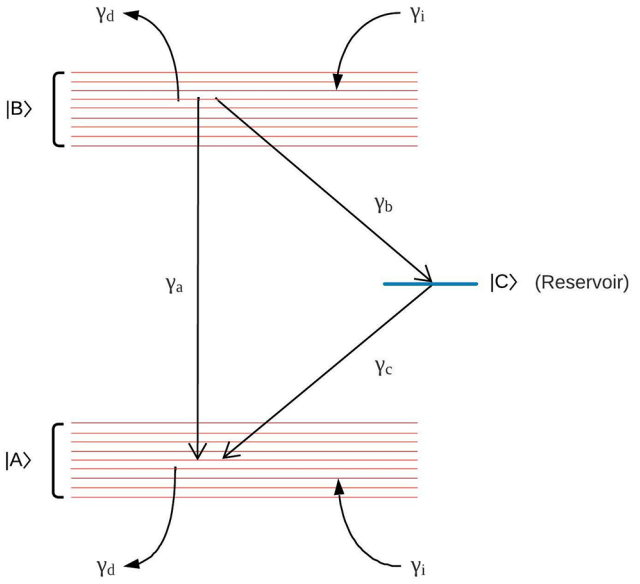

Figure 2. Two-state quantum system |A⟩, |B⟩ with internal relaxation and a reservoir state |C⟩. We place capital letters to emphasize that the ground and excited states are broadened.

the different forms in which the solvent encloses the dye molecule and to the different molecular configurations adopted by the latter. Mourou proposed that, due to the solute−solvent interaction, it occurs that randomly each molecule of the solvent enclosing the solute and each molecule of the solute adopt a new configuration involving a different transition frequency for the supermolecules. The inverse spectral diffusion rate γ_i from a defined frequency to the other states of the same band is given by $\gamma_i = g(\omega_0)/T_3$, where T_3 is the time required to change the transition frequency in a supermolecule, and it is hypothesized that, for a supermolecule, the rate of change from frequency ω_0 to ω_0' per unit frequency is proportional to the frequency distribution $g(\omega_0)$. This process is quantifiable with the decay rate from a defined state to other states within the same band, given by

$$\gamma_d = \int_0^\infty \gamma_i \, d\omega_0 = \int_0^\infty g(\omega_0)/T_3 d\omega_0 = 1/T_3 \tag{17}$$

In the study of the optical properties of quantum systems interacting with radiation, two types of systems are distinguished: closed and open. Closed is one in which any population leaving the upper state decays to the lower state: $\dot{\rho}_{aa} + \dot{\rho}_{bb} = 0$.

Open, the base and excited states can exchange population with associated reservoir states. In this case, the total population between the reservoir and the system is considered constant, expressed as $\rho_{aa} + \rho_{bb} + \rho_{cc} = g(\omega_0)$. Here, ρ_{cc} is the population of the reservoir state and does not correspond to an element of the density matrix.

2.2.2. Three-State Quantum System with Internal Relaxation: S_{3S}. Here, we consider a closed three-state quantum system incorporating spectral diffusion (Figure 3). Like the two-state system, both the excited and the ground state are considered to correspond to bands characterized by a broadening, subject to a frequency distribution defined by a Lorentzian. Yajima et al.[8] considered the MCG and the DQCI as three-state quantum systems. The results presented in these works showed that considering additional levels to those coupled with the FWM signal provides corrections to previous results. Due to these results and the fact that in nonideal

https://doi.org/10.1021/acsomega.2c07300
ACS Omega 2023, 8, 10690−10712

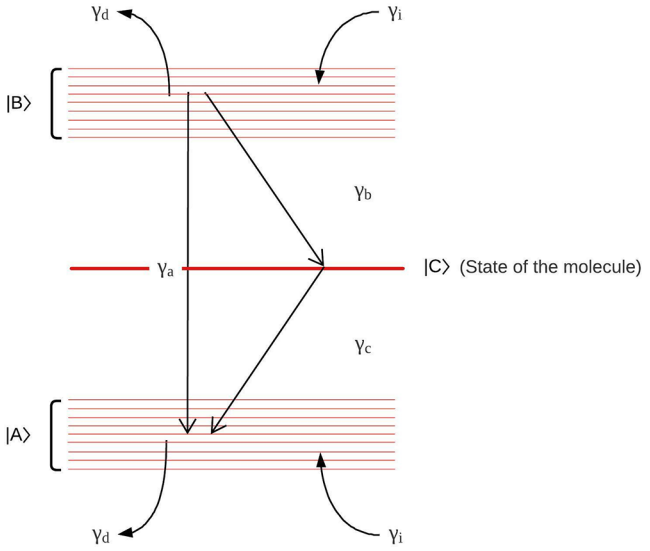

Figure 3. Three-state quantum system incorporating internal relationship:$\mathbf{S_{3S}}$.

materials it is usual that additional energy levels exist between the base and excited states, which are connected to the |A⟩, |B⟩ states through relaxation processes, the insertion of a third state in the quantum system is justified. Here the |A⟩ → |C⟩ and |B⟩ → |C⟩ transitions are far from resonance with the transition |A⟩ → |B⟩. In this scheme it is valid: $\dot{\rho}_{aa} + \dot{\rho}_{bb} + \dot{\rho}_{cc} = 0$

We proceed to consider the relaxation channels according to each quantum model, that is, to study the characteristics of the reservoir state and the spectral diffusion mechanisms. According to these general relaxation mechanisms and those of spectral diffusion, we can formulate the OCBEs in both study systems.

(a) Optical Conventional Bloch Equations for systems: S_{2S}^{R}

$$\frac{d\rho_{aa}}{dt} = -\frac{i}{\hbar}(H_{ab}\rho_{ba} - \rho_{ab}H_{ba}) + \gamma_a\rho_{bb} + \gamma_c\rho_{cc} - \frac{\rho_{aa}}{T_3} + [g(\omega_0)/T_3]\int_0^\infty \rho_{aa}(\omega'_0, t)\, d\omega'_0 \tag{18a}$$

$$\frac{d\rho_{bb}}{dt} = -\frac{i}{\hbar}(H_{ba}\rho_{ab} - \rho_{ba}H_{ab}) - \gamma_b\rho_{bb} - \gamma_a\rho_{bb} - \frac{\rho_{bb}}{T_3} + [g(\omega_0)/T_3]\int_0^\infty \rho_{bb}(\omega'_0, t)\, d\omega'_0 \tag{18b}$$

$$\frac{d\rho_{ba}}{dt} = \frac{d\rho_{ab}^*}{dt} = -\frac{i}{\hbar}(H_{ba})(\rho_{aa} - \rho_{\partial}) - (\Gamma_2 + i\omega_0)\rho_{ba} \tag{18c}$$

(b) Optical Conventional Bloch equations for systems: S_{3S}

$$\frac{d\rho_{aa}}{dt} = -\frac{i}{\hbar}(H_{ab}\rho_{ba} - \rho_{ab}H_{ba} + H_{ac}\rho_{ca} - \rho_{ac}H_{ca}) + \gamma_a\rho_{bb} + \gamma_c\rho_{cc} - \frac{\rho_{aa}}{T_3} + [g(\omega_{ab})/T_3]\int_0^\infty \rho_{aa}(\omega'_{ab}, t)d\omega'_{ab} \tag{19a}$$

$$\frac{d\rho_{bb}}{dt} = -\frac{i}{\hbar}(H_{ba}\rho_{ab} - \rho_{ba}H_{ab} + H_{bc}\rho_{cb} - \rho_{bc}H_{cb}) - (\gamma_a + \gamma_b)\rho_{bb} - \frac{\rho_{bb}}{T_3} + [g(\omega_{ab})/T_3]\int_0^\infty \rho_{bb}(\omega'_{ab}, t)d\omega'_{ab} \tag{19b}$$

$$\frac{d\rho_{cc}}{dt} = -\frac{i}{\hbar}(H_{ca}\rho_{ac} - \rho_{ca}H_{ac} + H_{cb}\rho_{bc} - \rho_{cb}H_{bc}) - \gamma_c\rho_{cc} + \gamma_b\rho_{bb} \tag{19c}$$

$$\frac{d\rho_{ba}}{dt} = -\frac{i}{\hbar}(H_{ba}(\rho_{aa} - \rho_{bb}) + H_{ba}\rho_{ca} - \rho_{bc}H_{ca}) - (\Gamma_{ba} + i\omega_{ba})\rho_{ba} \tag{19d}$$

$$\frac{d\rho_{ca}}{dt} = -\frac{i}{\hbar}(H_{ca}(\rho_{aa} - \rho_{cc}) + H_{cb}\rho_{ba} - \rho_{cb}H_{ba}) - (\Gamma_{ca} + i\omega_{ca})\rho_{ca} \tag{19e}$$

$$\frac{d\rho_{bc}}{dt} = -\frac{i}{\hbar}(H_{bc}(\rho_{cc} - \rho_{bb}) + H_{ba}\rho_{ac} - \rho_{ba}H_{ac}) - (\Gamma_{bc} + i\omega_{bc})\rho_{bc} \tag{19f}$$

$$\frac{d\rho_{jk}}{dt} = \frac{d\rho_{kj}^*}{dt} \quad (k, j = a, b, c) \tag{19g}$$

2.2.3. Resolutions of the OCBE, Calculations of Induced Polarizations, and Electrical Susceptibilities in Systems: S_{2S}^{R}. For this set of eqs 18a, the longitudinal decay time $T_1 \equiv \gamma_a^{-1}$ corresponds to the average time in which the molecules decay |B⟩ → |A⟩, γ_b is the de-excitation rate |B⟩ → |C⟩, γ_c is the de-excitation rate |C⟩ → |A⟩, while $T_2 \equiv \Gamma_2^{-1}$. Considering the dipolar-electric Hamiltonian: $H_{ba} = H_{ab}^* = -\mu_{ab}(E_1 e^{-i\omega_1 t} + E_2 e^{-i\omega_2 t}$ + cc). To advance in the calculation, it is necessary to solve in frequency space, and considering a perturbative scheme for the treatment of coherences and populations, according to $\rho_{ba}^{(3)}$, $\rho_{aa}^{(2)}$, $\rho_{bb}^{(2)}$, $\rho_{ba}^{(1)}$. Defining: $\Gamma_x = \Gamma_3 + \gamma_c$; $\Gamma_D = \gamma_a - \gamma_c$; $G_{\omega_j} = \int_0^\infty \rho_{bb}^{(2)}(\omega_j)d\omega'_0$; $I_{\omega_j} = \int_0^\infty \rho_{aa}^{(2)}(\omega_j)d\omega'_0$, we obtain

$$D_3\rho_{ba}^{(3)}(\omega_3) = -i\Omega_1(\rho_{aa}^{(2)}(\Delta) - \rho_{bb}^{(2)}(\Delta)) \tag{20}$$

$$(\Gamma_s - i\Delta)\rho_{bb}^{(2)}(\Delta) = -i[\Omega_1\rho_{ab}^{(1)}(-\omega_2) - \Omega_2^*\rho_{ba}^{(1)}(\omega_1)] + \frac{g(\omega_0)}{T_3}G_\Delta \tag{21}$$

with $\Gamma_s = \gamma_a + \gamma_b + T_3^{-1}$

$$(\Gamma_x - i\Delta)\rho_{aa}^{(2)}(\Delta) = -i[\Omega_2^*\rho_{ba}^{(1)}(-\omega_2) - \Omega_1\rho_{ab}^{(1)}(-\omega_2)] + \Gamma_D\rho_{bb}^{(2)}(\Delta) + \frac{g(\omega_0)}{T_3}I_\Delta + \gamma_c g^\Delta(\omega_0) \tag{22}$$

where $g^\Delta(\omega_0)$ is the component of the frequency distribution function that contributes the population of state |B⟩ when the detuning frequency of the FWM signal is Δ and its value is depreciable because it corresponds to a fixed event in a continuous probability distribution. Solving we have

$$D_2\rho_{ba}^{(1)}(\omega_2) = -i\Omega_2\rho_D^{(0)} \text{ and } \rho_{ab}^{(1)}(-\omega_j) = \rho_{ba}^{*(1)}(\omega_j) \tag{23}$$

https://doi.org/10.1021/acsomega.2c07300
ACS Omega 2023, 8, 10690−10712

Explicitly solving each perturbative term, we are left with

$$\rho_{bb}^{(2)}(\Delta) = \frac{\Omega_1\Omega_2^*\rho_D^{(0)}}{\Gamma_s - i\Delta}\left(\frac{1}{D_2^*} + \frac{1}{D_1}\right) + \frac{g(\omega_0)G_\Delta}{T_3(\Gamma_s - i\Delta)} \quad (24)$$

Replacing eq 24 in G_{ω_j}, we have

$$G_\Delta = \frac{\Omega_1\Omega_2^*\rho_D^{(0)}}{\Gamma_s - \Gamma_3 - i\Delta}J \text{ with } J = \int_0^\infty \left(\frac{1}{D_2^*} + \frac{1}{D_1}\right)d\omega_0 \quad (25)$$

Calculating this integral, we have $J = i \ln \frac{\Gamma_2^2 + \omega_2^2}{\Gamma_2^2 + \omega_1^2} + \tan^{-1}\frac{\omega_2}{\Gamma_2} + \tan^{-1}\frac{\omega_1}{\Gamma_2}$ and considering the approximation $\omega_1, \omega_2 \gg \Gamma_2$, we are left with $J \approx \pi$. Finally, for $\rho_{bb}^{(2)}(\Delta)$, we have

$$\rho_{bb}^{(2)}(\Delta) = \frac{\Omega_1\Omega_2^*\rho_D^{(0)}}{\Gamma_s - i\Delta}\left(\frac{1}{D_2^*} + \frac{1}{D_1}\right) + \frac{g(\omega_0)J}{T_3(\Gamma_s - i\Delta)} \quad (26)$$

$$(\Gamma_x - i\Delta)\rho_{aa}^{(2)}(\Delta) = \frac{\Omega_1\Omega_2^*\rho_D^{(0)}}{\Gamma_s - i\Delta}\left[\left(\frac{1}{D_2^*} + \frac{1}{D_1}\right)(\Gamma_D - \Gamma_s + i\Delta) + \frac{\Gamma_D J g(\omega_0)\Gamma_3}{\Gamma_s - \Gamma_3 - i\Delta}\right] + \frac{g(\omega_0)}{T_3}I_\Delta \quad (27)$$

Replacing eq 27 in I_{ω_j}, we have

$$I_\Delta = \frac{\Omega_1\Omega_2^*\rho_D^{(0)}J}{(\Gamma_x - i\Delta - \Gamma_3)(\Gamma_s - i\Delta)}\left[(\Gamma_D - \Gamma_s + i\Delta) + \frac{\Gamma_D\Gamma_3}{(\Gamma_s - \Gamma_3 - i\Delta)}\right] \quad (28)$$

Replacing eq 28 in eq 27, we obtain

$$\rho_{aa}^{(2)}(\Delta) = \frac{\Omega_1\Omega_2^*\rho_D^{(0)}}{(\Gamma_s - i\Delta)(\Gamma_x - i\Delta)}\left\{\left(\frac{1}{D_2^*} + \frac{1}{D_1}\right)(\Gamma_D - \Gamma_s + i\Delta) + Jg(\omega_0)\Gamma_3\Gamma_T\right\} \quad (29)$$

where

$$\Gamma_T = \frac{\Gamma_D}{\Gamma_s - \Gamma_3 - i\Delta} + \frac{1}{\Gamma_x - \Gamma_3 - i\Delta}\left[(\Gamma_D - \Gamma_s + i\Delta) + \frac{\Gamma_D\Gamma_3}{\Gamma_s - \Gamma_3 - i\Delta}\right]$$

.

In this way, we can finally[54] calculate the Fourier component of the coherence with frequency ω_3:

$$\rho_{ba}^{(3)}(\omega_3) = -\frac{i|\vec{\mu}_{ba}|^2\vec{\mu}_{ba}E_1^2E_2^*\rho_D^{(0)}}{\hbar^3 D_3(\Gamma_3 + \gamma_a + \gamma_b - i\Delta)}\left\{\left(\frac{1}{D_1} + \frac{1}{D_2^*}\right)\phi_1 + g(\omega_0)\phi_2\right\}$$

$$\phi_1 = \left(2 + \frac{\gamma_b}{\gamma_c + \Gamma_3 - i\Delta}\right)$$

$$\phi_2 = 2\pi\Gamma_3\left(\frac{\Delta^2 + i\Delta(\gamma_b + \Gamma_3 + 2\gamma_c) - \gamma_c(\gamma_c + \Gamma_3) - \frac{\gamma_b}{2}(\gamma_b + \gamma_a + \Gamma_3 + \gamma_c)}{(\gamma_c - i\Delta)(\gamma_a + \gamma_c - i\Delta)(\Gamma_3 + \gamma_c - i\Delta)}\right) \quad (30)$$

Eq 30 is responsible for the macroscopic polarization and nonlinear optical responses for the two-state quantum system of molecule in the presence of a reservoir state. As a particular case, without taking the reservoir state, making $\gamma_b \to 0$ and $\gamma_c \to 0$, we obtain

$$\rho_{ba}^{(3)}(\omega_3)|_{Yajima} = -\frac{2i|\vec{\mu}_{ba}|^2\vec{\mu}_{ba}E_1^2E_2^*\rho_D^{(0)}}{\hbar^3 D_3(\Gamma_3 + T_1^{-1} - i\Delta)}\left\{\left(\frac{1}{D_1} + \frac{1}{D_2^*}\right) + \frac{g(\omega_0)J\Gamma_3}{T_1^{-1} - i\Delta}\right\} \quad (31)$$

coincident with that proposed by Yajima et al.[8] Considering eq 31, we can determine the nonlinear polarization induced to third order

$$P^{(3)}(\omega_3) = N\int_0^\infty (\mu_{ab}\rho^{(3)}(\omega_3, \omega_0, t) + cc)d\omega_0 \quad (32)$$

and with it the electrical susceptibility using the tensor approximation, according to

$$\chi^{(3)}(\omega_3) = -\frac{iA(If_2 + I_1g_2)}{\Gamma_3 + \gamma_a + \gamma_b - i\Delta} \quad (33)$$

Here, we have defined $A = N|\mu_{ba}|^4\rho_D^{(0)}/\hbar^3$; $I = \int_0^\infty D_3^{-1}[D_1^{-1} + (D_2^*)^{-1}]d\omega_0 \approx \frac{\pi}{\Gamma_2 - i\Delta}$

$$I_1 = \int_0^\infty \frac{g(\omega_0)}{D_3}d\omega_0 \approx ig(\omega_3)\left\{\frac{1}{2}\ln\frac{\omega_3^2}{\Gamma_4^2 + \omega_c^2} - \frac{\omega_c - \omega_3 - i\Gamma_2}{\Gamma_4}\left[\frac{\pi}{2}\tan^{-1}\frac{\omega_c}{\Gamma_4}\right]\right\}$$

$$f_2 = 2 + \frac{\gamma_b}{\Gamma_3 + \gamma_c - i\Delta}$$

$$g_2 = -\{[2\pi\Gamma_3[\Delta^2 + i\Delta(\Gamma_3 + 2\gamma_c + \gamma_b) - \gamma_c(\gamma_c + \Gamma_3) - \frac{\gamma_b}{2}(\Gamma_3 + \gamma_a + \gamma_b + \gamma_c)]]/[(\gamma_c - i\Delta)(\gamma_a + \gamma_c - i\Delta)(\Gamma_3 + \gamma_c - i\Delta)]\}$$

To visualize solvent effects requires that the absorption band be sufficiently broad compared to the kinetic constants of the system.

2.2.4. Optical Bloch Equation Resolutions, Calculations of Induced Polarizations, and Electrical Susceptibilities in Systems: S_{3S}. Considering that now the state $|C\rangle$ of the reservoir for system S_{2S}^R will be considered as a proper state of the system under study (S_{3S}) taking into account the incorporation of spectral diffusion. In the system of eqs 19a, the $|C\rangle$ state away from the resonance with frequency ω_{ab} is considered, therefore, in the resolution of the differential equations corresponding to ρ_{ac} and ρ_{bc} the terms oscillating at frequencies $\omega_{bc} \pm \omega_j$ ($j = 1, 2, 3$) are eliminated in a similar way to that established in RWA. Following procedures like those presented in the previous section, we have for the Fourier component at the FWM frequency, the expression:

https://doi.org/10.1021/acsomega.2c07300
ACS Omega 2023, 8, 10690−10712

$$[\Gamma_{ba} + i(\omega_{ba} - \omega_3)]\rho_{ba}^{(3)}(\omega_3) = -\frac{i}{\hbar}[H_{ba}(\rho_{aa}^{(2)}(\Delta) - \rho_{bb}^{(2)}(\Delta))] \tag{34a}$$

Hence, the second order terms are given by

$$(\Gamma_3 + \gamma_a + \gamma_b - i\Delta)\rho_{bb}^{(2)}(\Delta) = i[\Omega_1\rho_{ab}^{(1)}(-\omega_2) - \Omega_2^*\rho_{ba}^{(1)}(\omega_1)] + \frac{g(\omega_{ab})}{T_3}G_\Delta \tag{34b}$$

$$(\Gamma_3 - i\Delta)\rho_{aa}^{(2)}(\Delta) = i[\Omega_2^*\rho_{ba}^{(1)}(\omega_1) - \Omega_1\rho_{ab}^{(1)}(-\omega_2)] + \gamma_b\rho_{bb}^{(1)}(\Delta) + \gamma_c\rho_{cc}^{(1)}(\Delta) + \frac{g(\omega_{ab})}{T_3}I_\Delta \tag{34c}$$

$$\rho_{cc}^{(2)}(\Delta) = \frac{\gamma_b}{\gamma_c - i\Delta}\rho_{bb}^{(2)}(\Delta) \tag{34d}$$

$$\rho_{ba}^{(1)}(\omega_1) = \frac{i\Omega_1\rho_D^{(0)}}{D_1} \tag{34e}$$

$$\rho_{ab}^{(1)}(-\omega_2) = -\frac{i\Omega_2^*\rho_D^{(0)}}{D_2^*} \tag{34f}$$

where $G_{\omega_j} = \int_0^\infty \rho_{bb}^{(2)}\omega_j(\omega_0')\mathrm{d}\omega_0'$ and $I_{\omega_j} = \int_0^\infty \rho_{aa}^{(2)}\omega_j(\omega_0')\mathrm{d}\omega_0'$. With a procedure like the one developed above, we evaluate G_Δ. Replacing eq 34e and 34f in 34b, and integrating the resulting equation:

$$G_\Delta = \frac{|\mu_{ba}|^2\rho_D^{(0)}E_1E_2^*}{(\gamma_a + \gamma_b - i\Delta)\hbar^2}J \tag{35}$$

Therefore, the term $\rho_{bb}^{(2)}(\Delta)$ is defined as follows:

$$\rho_{bb}^{(2)}(\Delta) = \frac{|\mu_{ba}|^2\rho_D^{(0)}E_1E_2^*}{\hbar^2(\gamma_a + \gamma_b + \Gamma_3 - i\Delta)}\left\{\left(\frac{1}{D_1} + \frac{1}{D_2^*}\right) + \frac{g(\omega_{ab})\Gamma_3}{(\gamma_a + \gamma_b - i\Delta)}J\right\} \tag{36}$$

and replacing eq 36 in eq 34d, we determine $\rho_{cc}^{(2)}(\Delta)$:

$$\rho_{cc}^{(2)}(\Delta) = \frac{|\mu_{ba}|^2\rho_D^{(0)}\gamma_bE_1E_2^*}{\hbar^2(\gamma_a + \gamma_b + \Gamma_3 - i\Delta)(\gamma_c - i\Delta)}\left\{\left(\frac{1}{D_1} + \frac{1}{D_2^*}\right) + \frac{g(\omega_{ab})\Gamma_3}{(\gamma_a + \gamma_b - i\Delta)}J\right\} \tag{37}$$

By replacing eqs 34e and 34f in eq 34c and integrating, the resulting equation:

$$I_\Delta = \frac{\Omega_1\Omega_2^*\rho_D^{(0)}J}{(-i\Delta)}\left[\left(\gamma_a + \frac{\gamma_c\gamma_b}{\gamma_c - i\Delta}\right)\left(\frac{1}{(\gamma_a + \gamma_b - i\Delta)} + \frac{\Gamma_3}{(\gamma_a + \gamma_b - i\Delta)(\gamma_a + \gamma_b + \Gamma_3 - i\Delta)}\right)\right]$$

This result of I_Δ, eqs 34e, 34f, 36, and 37, replaced in eq 34c, we obtain the matrix element $\rho_{aa}^{(2)}(\Delta)$, in the second order approximation:

$$\rho_{aa}^{(2)}(\Delta) = \frac{\Omega_1\Omega_2^*\rho_D^{(0)}}{(\gamma_a + \gamma_b + \Gamma_3 - i\Delta)(\Gamma_3 - i\Delta)}\left\{\left(\frac{1}{D_1} + \frac{1}{D_2^*}\right)R_\Delta - \frac{ig(\omega_{ab})\Gamma_3}{\Delta(\gamma_c - i\Delta)}JT_\Delta\right\} \tag{38}$$

where R_Δ and T_Δ are defined as

$$R_\Delta = \frac{(\Gamma_3 - i\Delta)(\gamma_c - i\Delta) - i\Delta\gamma_b}{(\gamma_c - i\Delta)}$$

$$T_\Delta = \frac{[\gamma_c(\gamma_a + \gamma_b) - i\Delta\gamma_a](\Gamma_3 - i\Delta)}{(\gamma_a + \gamma_b - i\Delta)} - (\Gamma_3 - i\Delta)(\gamma_c - i\Delta) + i\Delta\gamma_b$$

Finally, we obtain the coherence matrix element at the third order FWM frequency necessary to establish the induced polarization and the optical responses:

$$\rho_{ba}^{(3)}(\omega_3) = -\frac{i|\mu_{ba}|^2\mu_{ba}\rho_D^{(0)}E_1^2E_2^*}{D_3\hbar^3(\gamma_a + \gamma_b + \Gamma_3 - i\Delta)}\left\{\left(\frac{1}{D_1} + \frac{1}{D_2^*}\right)f_3 + g(\omega_{ab})g_3\right\} \tag{39}$$

where have defined: $f_3 = 2 + \frac{\gamma_b}{\gamma_c + \Gamma_3 - i\Delta + \frac{i\Gamma_3\gamma_c}{\gamma_c}}$ and

$$g_3 = -\frac{2\pi\Gamma_3\left[\Delta^2 + i\Delta(\Gamma_3 + \gamma_c + \gamma_b) - \gamma_c\Gamma_3 - \frac{\gamma_b}{2}(\Gamma_3 + \gamma_a + \gamma_b)\right]}{(\gamma_c - i\Delta)(\gamma_a + \gamma_b - i\Delta)(\Gamma_3 - i\Delta)}$$

It is possible to show that eq 39 in the presence of spectral diffusion for a three-state system converges to the result presented by Yajima et al.[8] in the case of a three-state quantum system, where both the ground and excited states are broadened into Lorentzian-described bands, when in the present model the internal relaxation is eliminated. That is

$$\rho_{ba}^{(3)}(\omega_3)|_{\text{Yajima}} = -\frac{i|\mu_{ba}|^2\mu_{ba}\rho_D^{(0)}E_1^2E_2^*}{D_3\hbar^3(\gamma_a + \gamma_b - i\Delta)}\left\{\left(\frac{1}{D_1} + \frac{1}{D_2^*}\right)\left(1 + \frac{\gamma_b}{2(\gamma_c - i\Delta)}\right)\right\} \tag{40}$$

Similarly, if we suppress all relaxation mechanisms with the solvent, eq 40 converges to the corresponding result presented for a simple model molecule, given by eq 2a. Through eq 39, we can evaluate the induced macroscopic nonlinear polarization, following schemes like those indicated above and evaluate in system S_{3S} in the presence of spectral diffusion. Expressing this polarization in tensor form, it is possible to calculate the third order electrical susceptibility in this system, according to the expression:

$$\chi^{(3)}(\omega_3) = -\frac{iA(If_3 + I_Lg_3)}{\Gamma_3 + \gamma_a + \gamma_b - i\Delta} \tag{41}$$

It is important to note the similarity of eq 41 in the three-state system with spectral diffusion and eq 33 for a system of two molecule states and a reservoir state. Although such expressions show this equivalence in form, the relaxation processes taking

https://doi.org/10.1021/acsomega.2c07300
ACS Omega 2023, 8, 10690−10712

place are conceptually different, as are the physical and molecular chemical systems to which they can be applied. The characteristic parameters used to present this graph were those suggested by several authors for organic dyes.[5,8,52] We have used the following parameters in MCG, according to $\gamma_a = \gamma_b = 10\gamma_c = \Gamma_2 = 9.09 \times 10^{12}$ s^{-1}. In Figure 4, the effect of decreasing

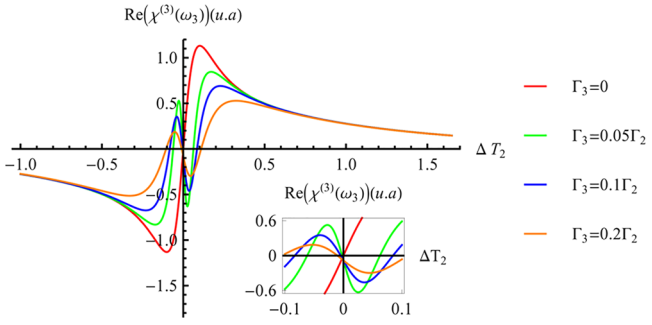

Figure 4. Real part of the nonlinear susceptibility as a function of detuning ΔT_2 frequency for different values of Γ_3 at $\gamma_a = \gamma_b = \gamma_c = \Gamma_2$ conditions for system S_{3S}. The inset shows an enlargement of the anomalous behavior in the nonlinear optical response just in the region of $|\Delta T_2| \leq 0.2$.

intensity of the nonlinear optical dispersive response as the spectral diffusion rate increases is maintained. However, the inset of Figure 4 shows an anomalous behavior detected in the expected dispersive response for the three-state quantum system. This anomalous behavior corresponds to an interference effect between the third eigenstate of the molecule and the spectral scattering. It is likely that this unexpected behavior in the behavior of the optical response just at the resonance maximum is due to the following factor:

$$i\Gamma_3\gamma_c/\Delta \tag{42}$$

which appears in eq 41, corresponding to the f_3 function of the nonlinear susceptibility. The factor shown appears due to the $-\gamma_\delta\rho_{cc}$ term arises from the quantum relaxation theory analysis applied to derive the optical Bloch equations.[38] It is important to note that this factor is zero when there is no spectral diffusion, i.e., when $\Gamma_3 = 0$ or when there is no third state of the molecule, $\gamma_c = 0$, and is amplified when $\Delta \approx 0$. Therefore, the anomalous effect shown in the "inset" arises only when a third eigenstate of the molecule and spectral diffusion in the near-resonance region are considered. It is possible to show from the above expressions that $g_i \ll f_i$. It is possible to note that this term (eq 42) is not contained in the quantum system S_{2S}^R because in that case, $|C\rangle$ being a reservoir state, its dynamics is determined by the $\rho_{aa} + \rho_{bb} + \rho_{cc} = g(\omega_0)$ ratio, this anomalous change predicts sudden changes in the nonlinear optical response for small variations of the detuning frequency, when it is close to zero, because it contains the Δ factor in its denominator. This behavior corresponds to a possible indication of potential applications in optical switches, given the abrupt change in the optical response.

Figure 5 shows the absorptive response of the three-state S_{3S} quantum system with spectral diffusion for the same characteristic parameters used in the previous figure. As in Figure 4, in this case there is an anomalous behavior in the absorptive response, shown in the inset of Figure 5, which is also attributed to the factor of eq 42. The effect shown in the inset of Figure 5 is a *hole burning* type effect, which usually arises when considering

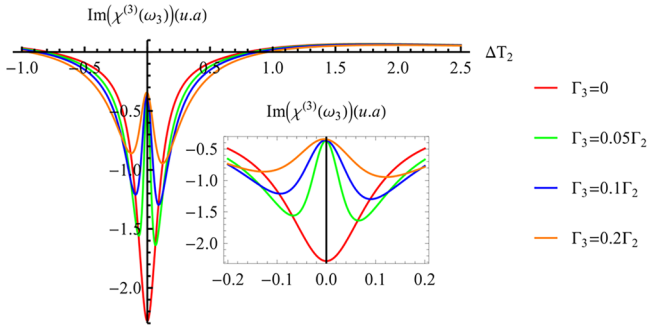

Figure 5. Imaginary part of the optical susceptibility as a function of the frequency detuning of the probe beam, for different values of Γ_3 when $\Gamma_a = \Gamma_b = \Gamma_2$ is satisfied. The inset shows an enlargement of the hole burning effect at S_{3S}.

saturative effects in the pumping beam; however, in this work, an effect of this type has been found in the absorption of the molecule only considering spectral diffusion and a third state of the molecule itself. It is important to note that, in both systems studied, the electrical susceptibility adopts the same functional form differentiated only in the functions f and g, with it being important that, in the absence of internal relaxation, where it is valid $\Gamma_3 \to 0$, and $f_2 = f_3 = 2 + \gamma_b/(\gamma_c - i\Delta)$, i.e., $g_2 = g_3 = 0$ in cases where spectral diffusion is not taken into account, the nonlinear absorptive and dispersive optical properties are independent of the nature of the third state considered.

To compare the effect of spectral diffusion in both semiclassical models, we have compared $|f_3/f_2|$ versus the detuning frequency. The intensity of the nonlinear optical responses for a S_{3S} system, in the region $\Delta \leq T_3$, decrease up to 70% as compared to the S_{2S}^R semiclassical system response. It means, in a degenerate-FWM process, the optical response of a S_{3S} system with cross-relaxation will be less intense than the response of a S_{2S}^R system for the same parameter values. It is important to note that our models S_{2S}^R and S_{3S} are designs of the molecular structure and its effect on the nonlinear optical responses, specifically on the FWM signal. All the above expressions converge exactly when we remove the $|C\rangle$ level in either of its two considerations and compact the bands to simple state levels, by not considering spectral diffusion.

2.3. Intramolecular Coupling. Intramolecular coupling corrects the wave functions of the Born−Oppenheimer (BO) approximation describing the molecule by altering the electric dipole moment. For more than half a century, research related to intramolecular coupling has made it possible to explain phenomena such as the so-called "forbidden" electronic transitions by symmetry in absorption aspects, or the molecular instability of molecular systems with configurations in electronically degenerate states according to the Jahn−Teller effect.[55]

Our work is concerned with including these intramolecular coupling details as a simplified description of the molecule. The vibronic coupling is of great importance in different chemical and physical processes; for instance, the study of this curve-crossing in weak transition probabilities forbidden by symmetry in absorption and emission processes.[56]

2.3.1. Coupled and Uncoupled Representations. In the adiabatic approximation the nuclear coordinates in space are considered fixed, introduced in the ψ_k-wave functions as parameters. However, the approximation becomes poor for vibrational states that are not too far separated from other states.[57] A more accurate approach to the wave functions

https://doi.org/10.1021/acsomega.2c07300
ACS Omega 2023, 8, 10690−10712

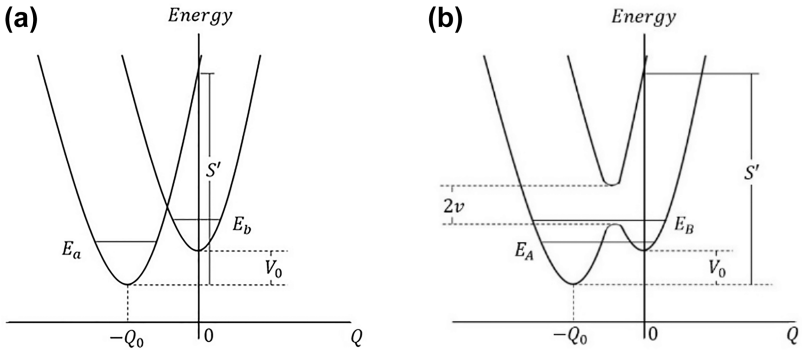

Figure 6. (a) Harmonic potentials displaced in nuclear coordinates by Q_0 and in energy by V_0; E_a and E_b are the energies of the fundamental vibrational states at each electronic level (coupled representation). (b) When the residual Hamiltonian $\tilde{H}$ is included. The energies for the vibrational levels are E_A and E_B (uncoupled representation).

characterizing a system with intramolecular interactions is the diabatic approximation, here, the electronic wave function is calculated for a specific fixed nuclear configuration Q_0 which does not necessarily refer to the actual position of the nucleus in space. Using Rayleigh−Schrödinger type perturbation theory the wave function is written as

$$\psi_i(r, Q) = \psi_i^{(0)}(r, Q_0) + \sum_{i\neq j} C_{ij}(Q)\psi_i^{(0)}(r,Q_0) \tag{43}$$

where

$$C_{ij}(Q) = \left[\langle\psi_i^{(0)}(r, Q_0)|\Delta U(r, Q)|\psi_j^{(0)}(r, Q_0)\rangle / \left(\varepsilon_j^0 - \varepsilon_i^0\right)\right] + \sum_{k\neq j}\left\{\langle\psi_i^{(0)}(r, Q_0)|\Delta U(r, Q)|\psi_k^{(0)}(r, Q_0)\rangle\langle\psi_k^{(0)}(r, Q_0)|\Delta U(r, Q)|\psi_j^{(0)}(r, Q_0)\rangle / \left[(\varepsilon_j^0 - \varepsilon_i^0)(\varepsilon_j^0 - \varepsilon_k^0)\right]\right\} + \ldots \tag{44}$$

and where the corrected total system wave function is

$$\psi_t(r, Q) = \left[\psi_i^{(0)}(r, Q_0) + \sum_{i\neq j} C_{ij}(Q)\psi_i^{(0)}(r,Q_0)\right]\chi_j(Q) \tag{45}$$

The eigenvalues of the electronic Hamiltonian of a molecular system determine the adiabatic potential energy surface (APES). The crossing of such surfaces implies a degeneracy in the energies, with values that depend on the nuclear coordinates.[58] The conic intersections are defined as singularities of the BO approximation.[59]

2.3.2. Molecular Model and Dipole Moments. The model to be used involves electronic states with potential curves described through harmonic curves shifted in both their nuclear and energy coordinates. We investigated modifications in the surfaces derived from the FWM signal by including simple schemes of the vibrational internal structure and all possible interactions because of vibronic coupling in situations where nonzero permanent dipole moments associated with the molecular electronic states are present (Figure 6a). The magnitude Q_0 represents the horizontal displacement, while V_0 represents the difference of the potential minima. The energies of the vibrational ground states are given by E_a and E_b and the vibrational functions by $\phi_{aj}(Q)$ and $\phi_{bk}(Q)$, respectively.

It is possible the inclusion of a residual perturbation, $\tilde{H}$, which allows the coupling of these electronic states, and consequently the curves described above, can now be separated according to the avoided crossover rule as shown in Figure 6b. The new generated eigenstates of the electronic Hamiltonian now belong to the so-called coupled representation, their form being dependent on the value of the nondiagonal matrix element of $\tilde{H}$ denoted in Figure 6b by v, the latter being the coupling parameter. Here, E_A and E_B denote the resulting vibronic energies after the inclusion of the coupling $\tilde{H}$, and the situation illustrated in Figure 6b corresponds to the situation where the diabatic image gives a good description of the vibronic states.

In our model, the two-electronic states are given by $\psi_a(q, Q)$ and $\psi_b(q, Q)$; the coordinate q and Q correspond to the electronic states and the nuclei coordinates, respectively. In our case, the isolated system is a two-level vibronic model based on harmonic potential curves. The Hamiltonian for the molecule is

$$H(q, Q) = H_0(q, Q) + \tilde{H}(q) \tag{46}$$

$H_0(q,Q) = T_q + T_Q + V(q,Q)$ corresponds to the vibrational scheme without a vibronic coupling. We have defined T_q and T_Q electronic and nuclear kinetic energy operators; $V(q,Q)$ is the potential energy, and finally, $\tilde{H}$ is a spin−orbit residual term dependence in electronic coordinates (q). The total wave function is expressed as

$$\Psi(q, Q) = C_{aj}\psi_a(q, Q)\phi_{aj}(Q) + C_{bk}\psi_b(q, Q)\phi_{bk}(Q) \tag{47}$$

in terms of a linear combination of two Born−Oppenheimer (BO) function; $\phi_{aj}(Q)$ and $\phi_{bk}(Q)$ have been defined as the vibrational states, $\psi_m(q,Q)$ (with $m = a, b$) are the electronic states. The diagonal elements of $\tilde{H}$ are the harmonic oscillators, while the nondiagonal elements represent the coupling between the two Born−Oppenheimer products. The inclusion of $\tilde{H}$ in the Hamiltonian system $H(q,Q)$ causes, from a geometrical point of view, that the two-potential energy curves in Figure 6a are separated and that the wave functions, as well as E_a and E_b change (Figure 6b). For the Hamiltonian $H(q,Q)$ of the system will be

$$H(q, Q)|\Psi_A\rangle = E_A|\Psi_A\rangle \tag{48a}$$

$$H(q, Q)|\Psi_B\rangle = E_B|\Psi_B\rangle \tag{48b}$$

The functions $|\Psi_A\rangle$ and $|\Psi_B\rangle$ of the uncoupled system are written using the BO approximation:$|\Psi_A\rangle = |\phi_{aj}\psi_a\rangle$, $|\Psi_B\rangle = |\phi_{bk}\psi_b\rangle$.

$$\langle\phi_{aj}\psi_a|H(q, Q)|\phi_{aj}\psi_a\rangle = E_{aj} = 2(j + 1/2) \tag{49a}$$

https://doi.org/10.1021/acsomega.2c07300
ACS Omega 2023, 8, 10690−10712

$$\langle \phi_{bk}\psi_b|H(q, Q)|\phi_{bk}\psi_b\rangle = E_{bk} = 2(k + 1/2) + V_0 \tag{49b}$$

The extra-diagonal elements are defined as the coupling produced by the residual Hamiltonian: $\langle \phi_{aj}\psi_a|\tilde{H}(q)|\phi_{bk}\psi_b\rangle = W_{ab}$ or $W_{ab} = \nu\langle \phi_{aj}|\phi_{bk}\rangle$, where we have defined $\nu = \langle \psi_a|\tilde{H}(q)|\psi_b\rangle$. In our case, we have defined the parameter ν as coupling-factor, while $\langle \phi_{aj}|\phi_{bk}\rangle$ is defined as the overlapping integral of vibrational wave functions. For the isolated system $H(q,Q)$ are given by

$$E_B = \frac{1}{2}\{(E_{aj} + E_{bk}) + [(E_{aj} + E_{bk})^2 - 4(E_{aj}E_{bk} - |W_{ab}|^2)]^{1/2}\} \tag{50a}$$

$$E_A = \frac{1}{2}\{(E_{aj} + E_{bk}) - [(E_{aj} + E_{bk})^2 - 4(E_{aj}E_{bk} - |W_{ab}|^2)]^{1/2}\} \tag{50b}$$

and where the wave function is given by the expression:

$$|\Psi_B\rangle = C_{jk}^B(\phi_{aj}\psi_a - D_{jk}^B\phi_{bk}\psi_b) \text{ and } |\Psi_A\rangle = C_{jk}^A(\phi_{aj}\psi_a - D_{jk}^A\phi_{ak}\psi_b) \tag{51}$$

where we have defined the coefficients as $C_{jk}^q = (1 + (D_{jk}^q)^2)^{-1/2}$ and $D_{jk}^q = (E_{aj} - E_q)/W_{ab}$ for values of q = A, B. In our models we have considered the following cases: $\nu \ll S'$, $\nu \approx S'$, and $\nu \gg S'$, where $S' = (m\tilde{\omega}_0/\hbar)Q_0^2$, and where m is defined as the reduced mass associated with the vibrational mode described by the coordinate Q; Q_0 is the separation between the two-minima of the electronic potentials. In our states, the Bohr frequency is defined as $\tilde{\omega}_0 = (E_A - E_B)/\hbar$. The permanent and transition dipole moments in the representations of the isolated molecule are given by

$$\mu_{BA} = \left[\frac{|W_{ab}|^2}{4|W_{ab}|^2 + \Delta^2}\right]^{1/2}\left[(m_{aa} - m_{bb}) - \frac{\Delta}{|W_{ab}|}m_{ab}\langle \phi_{aj}|\phi_{bk}\rangle\right] \tag{52}$$

In the diagonal case, $d = \mu_{BB} - \mu_{AA}$ is

$$d = \frac{\Delta(m_{aa} - m_{bb}) + 4|W_{ab}|m_{ab}\langle \phi_{aj}|\phi_{bk}\rangle}{\sqrt{\Delta^2 + 4|W_{ab}|^2}} = \frac{\Delta(m_{aa} - m_{bb}) + 4\nu m_{ab}\langle \phi_{aj}|\phi_{bk}\rangle^2}{\sqrt{\Delta^2 + 4\nu^2\langle \phi_{aj}|\phi_{bk}\rangle^2}} \tag{53}$$

m_{aa} and m_{bb} represent the permanent dipole moments corresponding to the $\psi_a(q,Q)$ and $\psi_b(q,Q)$ states in the coupled representation, respectively; $m_{ab}(-Q_0)$ is the transition dipole moment, while $m_{aa}(-Q_0)$ and $m_{bb}(0)$ are the permanent dipole moments. It is important to consider that when evaluating in this coordinate, we are referring to the Franck−Condon principle. The results shown in eqs 52 and 53 are the important quantities to take into consideration for the OCBE. For the overlapping integral, we have used the Pekarian formula:[60]

$$\langle \phi_{aj}|\phi_{bk}\rangle = \frac{(-1)^k}{(k!)^{1/2}}(S)'^{k/2}\exp(-S'/4)2^{-k/2} \tag{54}$$

It is important to note that with this new basis of calculation, the energies of the uncoupled states redefine the new Bohr frequency to be considered for the two-state system in the transition process associated with FWM, while the state functions in the same representation, allow the generation of new Rabi frequencies, which define the interaction process of the radiation with this new two-state system. Therefore, the polarization component at frequency $\omega_3 = 2\omega_1 - \omega_2$ is of the form:

$$\vec{P}(\omega_3) = N[\rho_{AB}(\omega_3)\vec{\mu}_{BA} + \rho_{BA}(\omega_3)\vec{\mu}_{AB} + \vec{d}\rho_{BB}(\omega_3) + \vec{\mu}_{AA}] \tag{55}$$

In the local case, the intensity of the nondegenerate FWM signal can be determined from $I_{FWM} \propto |\vec{P}(\omega_3)|^2$.

2.3.3. Density Matrix Elements in the Frequency Space: Local Considerations of Optical Length. Next, we describe in the presence of intramolecular coupling, the saturation effects coming from the pumping beam. We have treated the pump field at all perturbative orders, the probe and signal are considered at first order. In the case of explicitly considering permanent dipoles, it is necessary to incorporate oscillating terms at $\omega_n \pm \omega_m$ frequencies and leave the RWA without effect. Accordingly, one has for $\rho_{BA}(\omega_3)$ in the uncoupled basis:

$$\rho_{BA}(\omega_3) = \frac{\phi_2}{\phi_1}\rho_D^{dc} \tag{56}$$

$$\phi_2 = \left[\left(-\frac{2\Omega_1\Omega_2^*}{\Gamma_\Delta D_{\omega_1}^*} - \frac{2\Omega_2^*\Omega_1}{D_{\omega_1}\Gamma_{\omega_3}}\right)\Omega_1 - \frac{2|\Omega_1|^2\Omega_2^*}{\Gamma_\Delta\Gamma_{-\omega_2}^*} - \left(\frac{2\Omega_1^2}{\Gamma_\Delta D_{-\omega_2}} + \frac{\Omega_{d1}^2}{D_\Delta D_{-\omega_2}}\right)\Omega_2^*\right] \tag{56a}$$

https://doi.org/10.1021/acsomega.2c07300
ACS Omega 2023, 8, 10690−10712

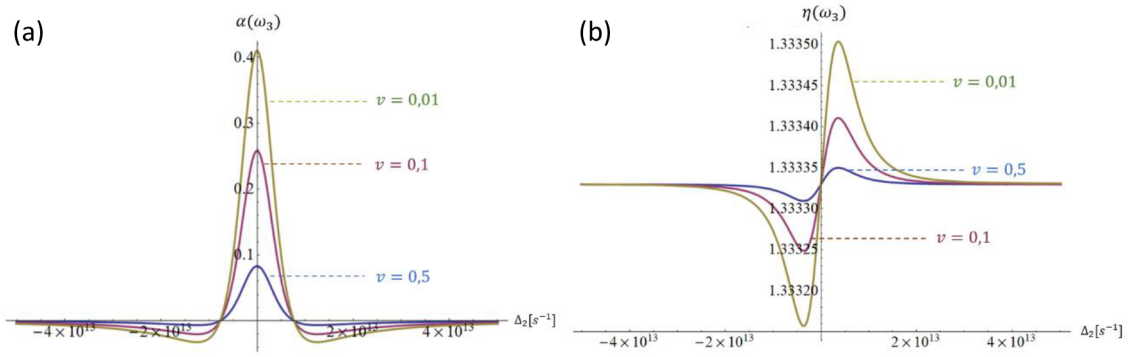

Figure 7. Absorptive (a) and dispersive (b) profiles of the organic dye Malachite green as a function of probe beam detuning for different values in the coupling parameter.

$$\phi_1 = \left\{ D_{\omega_3} + 2|\Omega_1|^2\left(\frac{1}{\Gamma_{\omega_1-\omega_2}} + \frac{1}{\Gamma_{3\omega_1-\omega_2}}\right) + |\Omega_{d1}|^2\left(\frac{1}{D_\Delta} + \frac{1}{D_{3\omega_1-\omega_2}}\right) + \right.$$
$$- 2i\frac{\Omega_1^*}{\Gamma_\Delta}\left[\left(-\frac{2|\Omega_1|^2\Omega_1^*}{\Gamma_\Delta D_{-\omega_2}^*} - \left(\frac{2|\Omega_1|^2}{\Gamma_\Delta D_{\omega_3}^*} + \frac{2|\Omega_1|^2}{\Gamma_{3\omega_1-\omega_2}D_{\omega_3}^*}\right)\Omega_1\right.\right.$$
$$\left.\left. - \left(\frac{2|\Omega_1|^2}{\Gamma_\Delta D_{-\omega_2}} + \frac{{\Omega_{d1}}^2}{D_\Delta D_{-\omega_2}}\right)\Omega_1^*\right)\right] + \frac{4i|\Omega_1|^2}{\Gamma_{3\omega_1-\omega_2}D_{\omega_3}^*}$$
$$\left(\frac{1}{\Gamma_\Delta} + \frac{1}{\Gamma_{3\omega_1-\omega_2}}\right)|\Omega_1|^2 + \frac{i\Omega_{d1}^*}{D_\Delta}\left[\left(\frac{2{\Omega_1}^2}{\Gamma_\Delta D_{\omega_2}} + \frac{{\Omega_{d1}}^2}{D_\Delta D_{-\omega_2}}\right)\right.$$
$${\Omega_{d1}}^* + \frac{2\Omega_1\Omega_{d1}}{D_\Delta\Gamma_{-\omega_2}}\Omega_1^* + 2\Omega_1^*\Omega_{d1}\Omega_1\left(\frac{1}{\Gamma_3 D_\Delta}\right.$$
$$\left.\left.\left. + \frac{1}{D_{\omega_3}D_{3\omega_1-\omega_2}}\right)\right] - \frac{i\Omega_1^*\Omega_{d1}}{D_{3\omega_1-\omega_2}}\left\{\left(\frac{-2\Omega_1^*\Omega_{d1}}{\Gamma_{\omega_3}D_\Delta}\right.\right.$$
$$\left.\left. + \frac{-2\Omega_1\Omega_{d1}^*}{D_{3\omega_1-\omega_2}D_{\omega_3}}\right) \right. \tag{56b}$$

$$\phi_3 = -i\left[\Omega_1\Omega_2^*\Omega_{d1}\left(\frac{1}{D_\Delta^* D_{-\omega_2}^*} + \frac{1}{D_{\omega_1}^* D_{2\omega_1}^*} - \frac{1}{D_\Delta D_{-\omega_2}}\right.\right.$$
$$\left.\left. - \frac{1}{D_{2\omega_1}D_{\omega_1}}\right) + {\Omega_1}^2\Omega_{d2}^*\left(\frac{1}{D_\Delta^* D_{\omega_1}^*} - \frac{1}{D_\Delta D_{\omega_1}}\right)\right]$$

where $D_{\mp m\omega_n} = {T_2}^{-1} - (\mp m\omega_n + \omega_0)$, $m = 1, 2, 3$ and $D_\Delta = {T_2}^{-1} - i(\Delta + \omega_0)$. Here, we define the population difference in the zero-frequency case as ρ_D^{dc}. The indicated result is a consequence of the saturation induced by the pumping beam, while the incidence of the coupling will be explicit when considering the dipole moments. In our treatments we will consider valid the fact that $\rho_{BA} = \rho_{AB}^*$, while $\rho_{BB}(\omega_3)$ is necessary to evaluate the polarization $P(\omega_3)$, which is given by

$$\rho_{BB}(\omega_3) = \frac{\phi_3}{\Gamma_{\omega_3}}\rho_D^{dc} \tag{57}$$

where

with $\Gamma_{\omega_3} = {T_1}^{-1} - i\omega_3$. In this perturbative case of the beams, the zero-frequency component is given by $\rho_D^{dc} = \rho_D^{(0)}\left[1 + \frac{4\tilde{S}}{{T_2}^2}\left(\frac{1}{D_{-\omega_1}D_{\omega_1}^*} + \frac{1}{D_{\omega_1}D_{-\omega_1}^*}\right)\right]$, with $\tilde{S}$ as the saturation parameter defined as $|\Omega_1|^2 T_1 T_2$. The Rabi frequencies associated with the transition and permanent dipole moments are defined as follows: $\Omega_n = (\vec{\mu}_{BA}\cdot\vec{E}_n(t))/\hbar$ and $\Omega_{dn} = (\vec{d}\cdot\vec{E}_n(t))/\hbar$ for $n = 1$, 2. For cases where the saturation effect of the pumping beam is maintained in molecular systems with zero permanent dipole moments in the uncoupled basis, we make $\Omega_{dn} = 0$, and in the ρ_D^{dc} component, the $D_{-\omega_1}$ term and $D_{-\omega_1}^*$ are absent. It is possible to derive from eqs 56 and 57 situations to the third order of total field by not explicitly considering the saturative processes that take place. In those cases, keeping situations of nonzero permanent dipole moments, the $\rho_{BA}^{(3)}(\omega_3)$ term is defined as

$$\rho_{BA}^{(3)}(\omega_3) = -\frac{2i{\Omega_1}^2\Omega_2^*}{D_{\omega_3}}\left(\frac{f_1}{J} + \frac{f_2}{\Gamma_{2\omega_1}}\right)\rho_D^{dc} - i\left(\frac{\Omega_{d1}}{D_{\omega_3}K}f_3 + \frac{\Omega_{d2}^*}{D_{2\omega_1}}f_4\right)\rho_D^{dc} \tag{58}$$

$$f_1 = \frac{1}{D_{-\omega_2}^*} + \frac{1}{D_{\omega_1}^*} + \frac{1}{D_{-\omega_2}} + \frac{1}{D_{\omega_1}}; f_2 = \frac{1}{D_{\omega_1}^*} + \frac{1}{D_{\omega_1}};$$
$$f_3 = \frac{\Omega_{d1}\Omega_2^*}{D_{-\omega_2}} + \frac{\Omega_1\Omega_{d2}^*}{D_{\omega_1}}; f_4 = \frac{\Omega_1\Omega_{d1}}{D_{\omega_1}}$$

$J = \Gamma_\Delta + 2|\Omega_1|^2\left(\frac{1}{D_{-\omega_2}^*} + \frac{1}{D_{-\omega_2}}\right)$ and $K = D_{\omega_1-\omega_2} + 2|\Omega_1|^2\left(\frac{1}{\Gamma_{-\omega_2}} + \frac{1}{D_{-\omega_2}}\right)$. In this case the diagonal component in $|B\rangle$ for the density matrix is given by

https://doi.org/10.1021/acsomega.2c07300
ACS Omega 2023, 8, 10690−10712

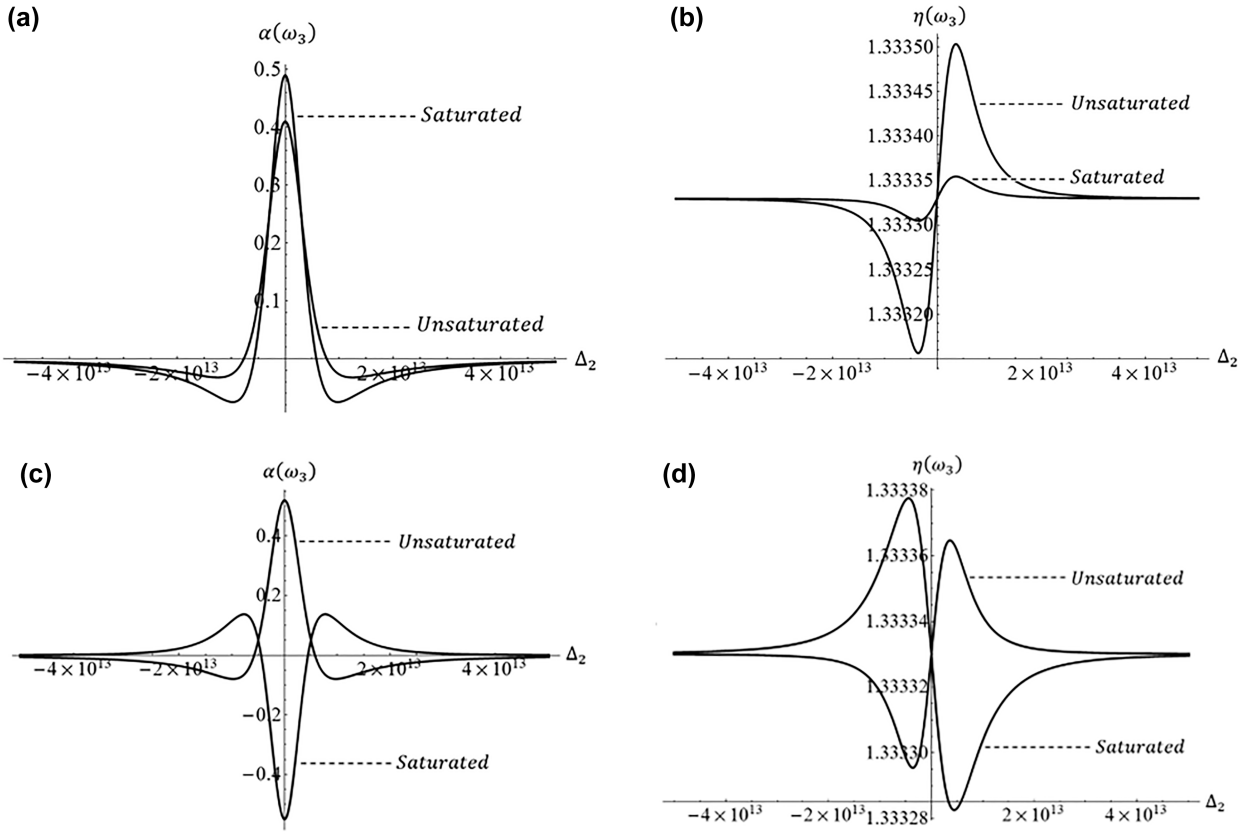

Figure 8. Absorptive (a) and dispersive (b) optical profiles when the permanent dipole moment is zero (a, b) in cases where pumping is considered saturative or in its third order perturbative scheme; (c, d) optical profiles in the presence of nonzero permanent dipole moments for equivalent intensity profiles.

$$\rho_{BA}^{(3)}(\omega_3) = -\frac{i\rho_D^{dc}}{\Gamma_{\omega_3}^*}\left[\frac{\Omega_1}{D_{\omega_1-\omega_2}^* + \frac{2|\Omega_1|^2}{\Gamma_{-\omega_2}} + \frac{|\Omega_{d1}|^2}{D_{-\omega_2}^*}} + \frac{\Omega_{d1}\Omega_2^*}{D_{-\omega_2}^*} + \frac{\Omega_1\Omega_{d2}^*}{D_{\omega_1}^*} + \frac{\Omega_1\Omega_{d1}\Omega_2^*}{D_{2\omega_1}^* D_{\omega_1}^*} - \left(\frac{\Omega_1}{D_{\omega_1-\omega_2} + \frac{2|\Omega_1|^2}{\Gamma_{-\omega_2}} + \frac{|\Omega_{d1}|^2}{D_{-\omega_2}}}\right)\left(\frac{\Omega_{d1}\Omega_2^*}{D_{-\omega_2}} + \frac{\Omega_1\Omega_{d2}^*}{D_{\omega_1}}\right) - \frac{\Omega_1\Omega_{d1}\Omega_2^*}{D_{2\omega_1}D_{\omega_1}}\right] \quad (59)$$

Finally, for situations of low pumping intensity and saturated system arguments with zero permanent dipole moments: it is necessary to evaluate $\rho_{BA}^{(3)}|_{d=0}$ and not to make $\rho_{BB}^{(3)}(\omega_3)$ related calculations because of the form that the $P^{(3)}(\omega_3)|_{d=0}$ polarization takes. In this case it is possible to observe that $J = \Gamma_\Delta$ and $f_2/\Gamma_{2\omega_1} \to 0$, $\rho_D^{dc} \to \rho_D^{(0)}$, while $f_3 = f_4 = 0$ and thus $\rho_{BA}^{(3)}(\omega_3)$ recovers the form stated in eq 2a. Considering the expressions for $\alpha(\omega_3)$ and $\eta(\omega_3)$, according to the saturative or perturbative processes, we can study their behavior subject to the effects of intramolecular coupling. We show in Figure 7, different absorption (Figure 7a), and scattering profiles (Figure 7b) as a function of detuning in the probe beam at different values of the coupling parameter. We observe how as the intramolecular coupling parameter becomes larger; the optical response profile decreases in intensity. This fact is linked to the separability of the system of uncoupled states from double minimum to single minimum potential curves. At low coupling values we expect the transitions to have greater strength because of their verticality to a fixed nuclear coordinate value.

Most likely increases in coupling reduce the transition strength given the diagonalization of the transition. Under considerations in both the saturation regimes and in the third order perturbative pumping scheme (unsaturated) we present Figure 8 for the nonlinear optical responses, choosing as a representative value of the intramolecular coupling of 0.01.

Figure 8 shows the change of the absorptive and dispersive optical responses as a function of detuning in the probe beam, considering the most probable transition between fundamental levels. Cases where there is saturation of part of the pumping, and where the latter is considered at second order according to perturbation theory, are studied. For these cases, the intramolecular coupling model is considered, for cases where the differences of the permanent dipole moments are zero and nonzero. It is remarkable that in the case where the pumping beam is treated by its saturation in the OCBEs, both the absorptive and dispersive intensity for the malachite green chloride molecule with intramolecular coupling, the intensity is higher. Curves a and b are associated with optical properties where the permanent dipole difference is zero. Curves c and d represent the optical responses for the case where that dipole difference is nonzero, contrasting between a strong pumping beam considering saturation and without such effects. For the

https://doi.org/10.1021/acsomega.2c07300
ACS Omega 2023, 8, 10690−10712

case of treatment to all orders in perturbation theory for the pumping beam, a higher magnitude of intensity tends to be generated in both optical responses, regardless of the null or not of the dipole moment differences, this, under vibronic considerations. We consider that the saturative effects cause a decrease in population at the fundamental level, generating a decrease in the absorption intensity. As a result, the absorptive and dispersive responses increase in intensity as the time to lose the coherence induced through the electric dipoles increases. In the absence of saturative effects, the lower level with a high population causes higher absorption at the transition. The saturation effects are mainly associated with a higher progression or transmission of the fields along their optical length in the material, thus indicating a low dispersion. It is important to note that in cases of nonzero permanent dipole difference and in the presence of saturation by pumping, the induced or transition dipoles change sign when considering the case of uncoupled representation. For absorptive cases it implies zero crossing, thus canceling the nondegenerate FWM signal. We can observe from the expressions, that the inclusion of intramolecular effects in the proposed semiclassical model modifies the corresponding eigenwave functions of the system and the existence of permanent dipoles in molecules with parity symmetry is admitted. There it has been represented in the detuning frequency space conformed by Δ_1,Δ_2 the intensity of the signal with the multiple resonances that take place and where it specifically studies the topology of the FWM signal and the sensitivity of the resonance peaks with these variables of the vibronic effect.

2.3.4. Propagation and High-Order Effects. Our proposal aims to explore how the FWM field propagates over a defined optical length, when simultaneously considering the saturative effects generated by the high-intensity beam and the molecular structure details associated with intramolecular coupling. From the results obtained it is remarkable the existing correlation of sensitivity in the optical response and the nature of the molecular structure. Additionally, the exponential dependence of the FWM signal on the pumping intensity, associating the fact to a parametric amplification that has been achieved with the tuning in the organic dye. By introducing a perturbative treatment for the reduce density matrix, relationships for the Fourier components of the $\tilde{\rho}_{BA}(\omega_k)$ and $\tilde{\rho}_D(k\Delta)$ in the $|A\rangle$, $|B\rangle$ uncoupled representation, are obtained:

$$L_{2n+1}\tilde{\rho}_{BA}(\omega_k) = i\tilde{\Omega}_2[(n+1)\Delta] + i\tilde{\Omega}_3[(n-1)\Delta] + i\tilde{\Omega}_1[n\Delta] \quad k = 1, 2, 3 \tag{60}$$

$$\begin{aligned}\Gamma_n(n\Delta)\tilde{\rho}_D(n\Delta) = &-2i\tilde{\Omega}_1\tilde{\rho}_{AB}[-(\omega_1 - n\Delta)] \\ &+ 2i\tilde{\Omega}_1^*\rho_{BA}[(\omega_1 + n\Delta)] - 2i\tilde{\Omega}_2\rho_{AB}\{-[\omega_1 - (n+1)\Delta]\} \\ &+ 2i\tilde{\Omega}_2\rho_{BA}[\omega_1 + (n-1)\Delta] - 2i\tilde{\Omega}_3 \\ &\rho_{AB}\{-[\omega_1 - (n-1)\Delta]\} + 2i\tilde{\Omega}_3\rho_{BA}[\omega_1 + (n+1)\Delta] \\ &+ \delta_{n,0}\tilde{\rho}_D^{(0)}\end{aligned} \tag{61}$$

where we have defined $L_{2n+1} = \tilde{T}_2^{-1} + i[\omega_0^{AB} - (n+1)\Delta]$, with $n = 0, 1, -1$ for pump, signal, and probe, respectively; whereby $L_{-1} = L_2$. Here, we have derived an effective transverse relaxation time which is a function of the parameters defining intramolecular coupling, given by

$$\frac{1}{\tilde{T}_2} = \frac{1}{T_2} + \frac{i}{\hbar}\left[\frac{V_0(m_{11} - m_{22}) - 4\nu e^{-S'/2}m_{22}}{(4\nu^2 e^{-S'/2} + V_0^2)}\right]E(t) \tag{62}$$

It is important to have noted eqs 60 and 61, since they define the Fourier components of the coherences and of the populations at the frequency in the presence of a signal field that is generated from the scattering process, but by considering the optical propagation length finite, this signal field now intervenes in the photonic processes, unlike what happens in local regimes, where only two incident beams are considered and the signal beam at the same frequency is measured in its intensity only at the local point. That is, the FWM signal is absorbed in the material, but participates in the scattering process with the other two incident beams. In the first approximation, we consider that $\mu_{AA} \approx \mu_{BB}$, without implying that the permanent dipole moments in the uncoupled basis $|1\rangle$,$|2\rangle$ are equal or equal to zero. We solved eqs 60 and 61 using perturbation theory: pump is treated to all orders, probe to second order, and FWM signal (generated) to first order. In this case, the generated coherences are of the form given by eq 3. In our models, it is possible to consider T_2 instead of $\tilde{T}_2$ because the approximation is valid: $4\nu^2 e^{-S/2}(4e^{-S/2}m_{ba}^2 - 1) \ll V_0^2$, for the case where $m_{aa} \approx m_{bb}$. Based on the diagonal and extra-diagonal density matrix elements, we evaluate the Fourier component associated with the induced nonlinear polarization through the expression $\vec{P}(\omega_k) = N\langle\tilde{\rho}_{BA}(\omega_k,\tilde{\omega}_0)\text{-}\vec{\mu}_{AB}\rangle_\theta$, where N is the chemical concentration of the active solute, while the bracket $\langle\cdots\rangle_\theta$ represents the average value the averaging over the possible molecular orientations. Considering the perturbative treatment where the test beam is evaluated to the second order, it is possible to make symmetrical all the expressions of envelopes of each of the fields in their propagation along the optical path. Considering that the pumping beam is highly intense, it is possible that in its optical path in the z-direction, its amplitude remains constant or varies exaggeratedly little. This allows us to express for the test beams and FWM signal:[40,46]

$$\frac{d\tilde{E}_3}{dz} = -\tilde{\alpha}_3(\omega_3)\tilde{E}_3 + \zeta_3\tilde{E}_2^*\exp(-i\Delta k_z z) \tag{63}$$

$$\begin{aligned}&\frac{d\tilde{E}_2^*}{dz} = -\tilde{\alpha}_2(\omega_3)\tilde{E}_2^* + \zeta_2^*\tilde{E}_3^*\exp(-i\Delta k_z z) \\ &\tilde{\alpha}_j(\omega_j) = \frac{2\pi\omega_j}{\eta_j c}Im(\chi^{(1)}(\omega_j)) \\ &\zeta_j = \frac{2\pi i\omega_j}{\eta_j c}\chi^{(3)}(\omega_j)\tilde{E}_1^2 \\ &\eta_j(\omega_j) = [1 + 4\pi Re\chi^{(1)}(\omega_j)]^{1/2}\end{aligned} \tag{64}$$

The coefficients ξ_2 and ξ_3 are the coupling parameters between the weak beams:

https://doi.org/10.1021/acsomega.2c07300
ACS Omega 2023, 8, 10690−10712

$$\chi^{(1)}(\omega_k) = \frac{|\mu_{BA}|^2 N}{\hbar} B_k \text{ and } \chi^{(3)}(\omega_k) = \frac{|\mu_{BA}|^2 N}{\hbar \tilde{E}_1^{\,2}} \kappa_i$$

$$B_3 = \frac{i\tilde{\rho}_D^{dc}}{2L_3}\left[\frac{\Gamma_1(\Delta) + 2|\tilde{\Omega}_1|^2\left(\frac{1}{L_2^*} + \frac{1}{L_1^*}\right)}{\Gamma_1(\Delta) + 2|\tilde{\Omega}_1|^2\left(\frac{1}{L_2^*} + \frac{1}{L_3}\right)}\right]$$

$$B_2^* = \frac{-i\tilde{\rho}_D^{dc}}{2L_2^*}\left[\frac{\Gamma_1(\Delta) - 2|\tilde{\Omega}_1|^2\left(\frac{1}{L_1} - \frac{1}{L_3}\right)}{\Gamma_1(\Delta) + 2|\tilde{\Omega}_1|^2\left(\frac{1}{L_2^*} + \frac{1}{L_3}\right)}\right]$$

$$\kappa_3 = \frac{-i\tilde{\Omega}_1^{\,2}\tilde{\rho}_D^{dc}}{L_3}\left[\frac{\left(\frac{1}{L_1} + \frac{1}{L_2^*}\right)}{\Gamma_1(\Delta) + 2|\tilde{\Omega}_1|^2\left(\frac{1}{L_1^*} + \frac{1}{L_3}\right)}\right]$$

$$\kappa_2^* = \frac{i\tilde{\Omega}_1^{\,2}\tilde{\rho}_D^{dc}}{L_2^*}\left[\frac{\left(\frac{1}{L_1^*} + \frac{1}{L_3}\right)}{\Gamma_1(\Delta) + 2|\tilde{\Omega}_1|^2\left(\frac{1}{L_2^*} + \frac{1}{L_3}\right)}\right]$$

$B_1 = \frac{i\tilde{\rho}_D^{dc}}{2L_1}$. Solving eqs 63 and 64, we get

$$\tilde{E}_3(z) = \frac{\zeta_3(\tilde{E}_2^{(0)})^*}{2K_{eff}}[e^{G_+z} - e^{G_-z}]\exp(i\Delta k_z z) \tag{65}$$

$$\tilde{E}_2^*(z) = \frac{(\tilde{E}_2^{(0)})^*}{2K_{eff}}\left\{\left(\frac{i\Delta k_z}{2} - \alpha_2\right)(e^{G_+z} - e^{G_-z}) - G_- e^{G_+z} + G_+ e^{G_-z}\right\}\exp(i\Delta k_z z) \tag{66}$$

where $K_{eff} = \frac{1}{2}[(\alpha_2 + \alpha_3 + i\Delta k_z) + 4\zeta_2^*\zeta_3]^{1/2}$. We highlight in the above expressions, the gain coefficient associated with the FWM process under the consideration of intramolecular effects, defined according to

$$G_\pm = \pm K_{eff} - \frac{1}{2}(\alpha_2 + \alpha_3) \text{ with } \Delta k_z \approx \frac{\omega}{c}((2\eta_1 - (\eta_2 + \eta_3)\cos\theta) \tag{67}$$

where the boundary conditions are given by $\tilde{E}_3(0) = 0$ and $\tilde{E}_2(0) = \tilde{E}_2^{(0)}$. Of eq 65, it is possible to obtain

$$\left|\frac{\tilde{E}_3(z)}{\tilde{E}_2^*(z)}\right|^2 = |\zeta_3(0)|^2 z^2 e^{-Ref(z)z}\sin^2(\theta)/\theta^2 \text{ with } \theta = \Delta k_z/2 \tag{68}$$

In this case, $f(z)$ is expressed as $f(z) = \alpha_2 + \alpha_3 - i\Delta k_z$ considering $4\zeta_3\zeta_2^* \ll (\Delta k_z)^2$. Since we propose to analyze the propagation process and its influence on the behavior of the nonlinear response, absorptive and dispersive optical processes in the FWM signal, and in the presence of intramolecular coupling, we then define the dipole moment in the $|A\rangle$, $|B\rangle$representation as a critical quantity in our analysis.

To this end, let us observe in Figure 9 how the transition moment changes as a function of intramolecular coupling, considering the moments in the coupled representation.

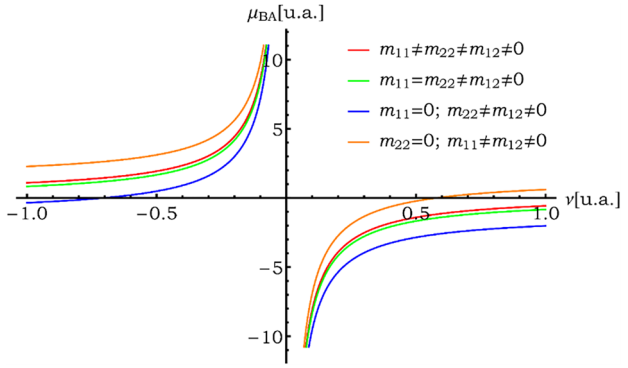

Figure 9. Analysis of the transition dipole moment in the uncoupled representation as a function of the intramolecular coupling parameter in different cases of ratio of the permanent and transition dipole moments in the coupled representation$|1\rangle$, $|2\rangle$.

It is remarkable to appreciate the hyperbolic shape of the dipole moments in the case of uncoupled representation, with divergences in the cases of null intramolecular coupling parameter. On the other hand, it is observed in Figure 10a, a pattern with a defined periodicity in the FWM signal intensity as its optical path progresses. Likewise, a decrease in FWM signal intensity within a specific period is shown as the structural coupling parameter increases, which can be seen from eq 68. On the other hand, Figure 10b shows that the intensity of the emerging FWM beam presents slight variations with respect to the coupling parameter, for the cases of weak pump perturbations, when these are expressed through the Rabi frequency. We note from eq 68 that the normalized FWM signal intensity with respect to the test intensity maintains an explicit dependence on both z and (Δk_z) detuning, unlike the implicit case with dependence on the molecular structure-dependent intramolecular coupling parameter. From Figure 10b we note that the dependence of the nonlinear FWM signal intensity on the pump intensity (expressed in terms of the square of the Rabi frequency) is of the exponential type, notably larger than the commonly observed linear dependence. From this fact, we can infer the existence of parametric amplifications[61] at these values of the optical path and for defined values of the coupling parameter, when tuned with organic dye such as MCG,[62] employed in our computational models. In Paz et al.[46] other studies have been realized for the evaluation of the intensity signal according at different z. In this last reference and through the results expressed there, we were able to derive an effective relaxation time $\tilde{T}_2$, with an explicit dependence on the parameters that characterize the intramolecular coupling. Our results on the propagation of the emerging fields, particularly the one associated with the Four-Wave mixing process, indicate that in the defined optical spacing, aperiodic structure with strictly localized maxima and minima is maintained, which can be checked to coincide with the structures shown by other authors as an experimental fact.[37]

2.4. Solvent Effect on Nonlinear Optical Responses: Stochastic Nature. In the previous sections, we have qualified the study systems with different models, emphasizing that the transitions between states are governed by Bohr $\tilde{\omega}_0$ frequencies that define the quantization of the states. In general terms or real-world situations, strictly radiative effects are not the only, let alone the most dominant, source of relaxation and coherence fluctuations, and depending on the type of you are, various modifications in the longitudinal and transversal relaxation times

https://doi.org/10.1021/acsomega.2c07300
ACS Omega 2023, 8, 10690−10712

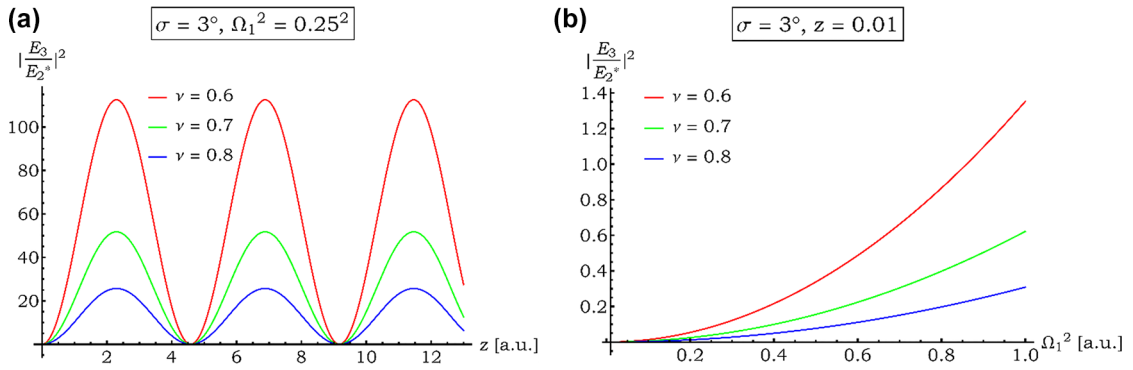

Figure 10. (a) Normalized intensities $|\tilde{E}_3(z)/\tilde{E}_2^*(z)|^2$ defined as a function of the optical path z at different values of the parameter defining the coupling (ν), with an angle of incidence ($\sigma = 3°$) between the pump and probe beams and a fixed value of the Rabi square frequency of the pump beam ($\tilde{\Omega}_1{}^2$); (b) normalized ratio of the FWM intensities as a function of the Rabi square frequency ($\tilde{\Omega}_1{}^2$) for different values of ν and a fixed value of z, with $\sigma = 3°$.

can take place. Stochastic type models are frequently employed, where collisions between the chemical actors (solute and solvent) induce shifts in the transition frequency and due to the intrinsic nature of the collision, can then lead to stochastically controlled modulations of the transition frequency between the states.[34] Wodkiewicz[63] has shown that in the presence of random fields, exact solutions exist and can be obtained for a set of differential equations of stochastic nature. We will include perturbative treatments, as well as saturation type schemes of the pumping beam, developments both in the time domain and in the frequency domain, even considering combinations of this stochastic description with intramolecular coupling scheme, measuring simultaneity of the effects.[64,65]

2.4.1. Stochastic Considerations in Nonlinear Optical Properties: FWM in Perturbative Regimes. Our model is based on describing the transition between molecular states through a Bohr frequency as a time-dependent function of stochastic nature, resulting from random collisions between the solute and the solvent.[66] The conventional optical Bloch equations can be viewed in two general limits. In the first of these, we consider non-Markovian type processes in the so-called impact approximation where the averaged components that have been perturbed by the thermal bath obey a strict set of differential equations. On the other hand, in cases where the relaxation mechanism involves changes in the frequency of the molecular transition, the nature of the equations governing the time development of the Bloch vector are of integro-differential form, and therefore, the validity of the OCBE is no longer possible. Already in ref 67, we have implemented a methodology based on perturbative treatments, considering the third order as the minimum order of existence of the four-wave mixing signal. This is,

$$\partial_t \rho_\xi = C_\xi(t)\rho_\xi(t) + R(t) \tag{69}$$

$$\rho_\xi(t) = \begin{pmatrix} \rho^{(3)}_{\xi,\mathrm{ba}} \\ \rho^{(2)}_{\xi,\mathrm{D}} \\ \rho^{(1)}_{\xi,\mathrm{ba}} \\ \rho^{(1)}_{\xi,\mathrm{ab}} \end{pmatrix}$$

$$C_\xi(t) = \begin{pmatrix} -\left(i\xi + \frac{1}{T_2}\right) & -\frac{i}{\hbar}(H_I)_{\mathrm{ba}} & 0 & 0 \\ 0 & -\frac{1}{T_1} & \frac{2i}{\hbar}(H_I)_{\mathrm{ab}} & -\frac{2i}{\hbar}(H_I)_{\mathrm{ba}} \\ 0 & 0 & -\left(i\xi + \frac{1}{T_2}\right) & 0 \\ 0 & 0 & 0 & \left(i\xi - \frac{1}{T_2}\right) \end{pmatrix}$$

$$R(t) = \begin{pmatrix} 0 \\ 0 \\ -\frac{i}{\hbar}(H_I)_{\mathrm{ba}} \\ \frac{i}{\hbar}(H_I)_{\mathrm{ab}} \end{pmatrix} \rho^{(0)}_{\mathrm{D}}$$

To solve eq 69, it is convenient to make explicit the form that the Hamiltonian operator must have and then solve the associated homogeneous equations. To do so, it is necessary to start at the lowest order (1) for the coherences, it is necessary to start at the lowest order (1) for the coherences $\rho^{(1)}_{\xi,\mathrm{ba}}(t)$ and $\rho^{(1)}_{\xi,\mathrm{ab}}(t)$. Once established, the second order term associated with the population differences must be solved $\rho^{(2)}_{\xi,\mathrm{D}}(t)$, and finally, the coherence at the frequency of FWM at the third order, given by $\rho^{(3)}_{\xi,\mathrm{ba}}(t)$. Once established, the second order term associated with the population differences must be solved, and finally, the coherence at the frequency of FWM at the third order. Finally, the third order coherence associated with the nondegenerate FWM signal, is given by

https://doi.org/10.1021/acsomega.2c07300
ACS Omega 2023, 8, 10690−10712

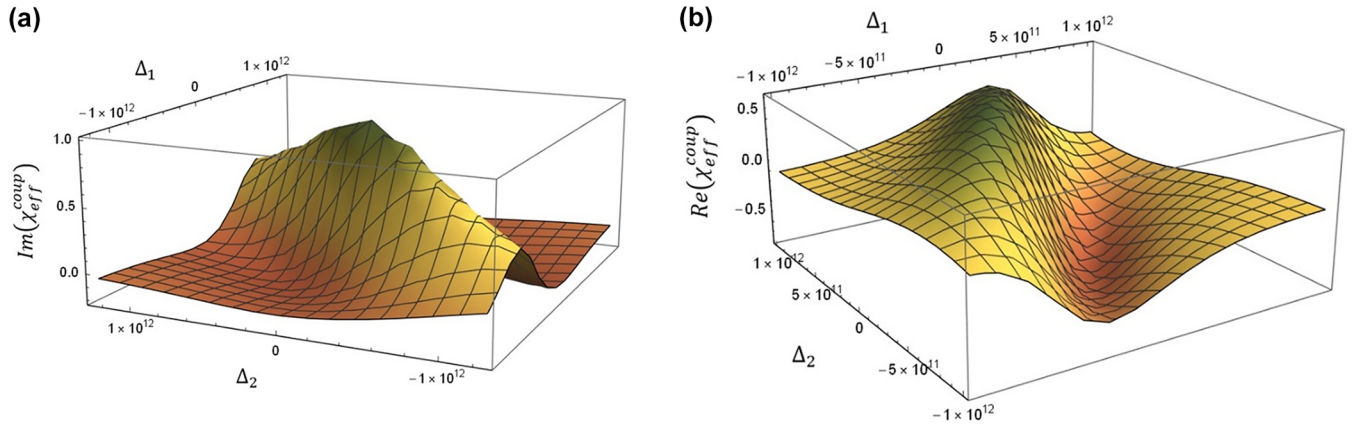

Figure 11. (a) Nonlinear absorption coefficient and (b) nonlinear refraction index as a function of pump- and probe-detuning in absence of noise for solvent, this is $\sigma(t) = 0$.

$$\rho_{\xi,\mathrm{ba}}^{(3)}(t) = 2i\Omega_1{}^2\Omega_2^*\rho_{\mathrm{D}}^{(0)}\exp\left(-\frac{t}{T_{,2}} + i(2\vec{k}_1 - \vec{k}_2)\cdot\vec{r}\right)$$
$$\int_{-\infty}^{t} \mathrm{d}x\ \exp(-xB_1)\int_{-\infty}^{x}\mathrm{d}z\ \exp(B_2 z)$$
$$\times\int_{-\infty}^{t}\mathrm{d}y\ \exp(A_1 y)\exp\left(\int_t^x i\xi(q)\mathrm{d}q\right)\exp\left(\int_z^y i\xi(s)\mathrm{d}s\right)$$
$$+\ 2i\Omega_1{}^2\Omega_2^*\rho_{\mathrm{D}}^{(0)}\exp\left(-\frac{t}{T_{,2}} + i(2\vec{k}_1 - \vec{k}_2)\cdot\vec{r}\right)$$
$$\int_{-\infty}^{t} \mathrm{d}x\ \exp(-xB_1)\int_{-\infty}^{x}\mathrm{d}z\ \exp(B_1^* z)$$
$$\times\int_{-\infty}^{t}\mathrm{d}y\ \exp(A_2^* y)\exp\left(\int_t^x i\xi(q)\mathrm{d}q\right)\exp\left(-\int_z^y i\xi(s)\mathrm{d}s\right) \tag{70}$$

where $A_k = \frac{1}{T_2} - i\omega_{\mathrm{k}}$; $B_k = \frac{1}{T_1} - A_{\mathrm{k}}$.

As shown in the above expressions, we have evaluated the averages in the set of realizations of the random variable. On this, van Kampen[65] has proposed solutions of these stochastic equations, considered equations of deterministic character, and subsequently took the stochastic averages. In our proposal, it has been possible to solve the stochastic OSBE equations in a perturbative way as if they were of deterministic nature equivalent to the OCBE and then the averaging of coherences in the realizations of the stochastic variable $\xi(t)$. Under the information that both $\rho_{\xi,\mathrm{ba}}^{(3)}(t)$ and $\rho_{\xi,\mathrm{ab}}^{(3)}(t)$ depend on the random variable, our model is based on taking those averages in the statistical set over the distribution of states with molecular frequencies in the interval between $\xi(t)$ and $\xi(t)+ \mathrm{d}\xi(t)$. From the expressions shown, we can see that the dependence on the variable $\xi(t)$ is exclusively located in the functions of the type: $\Psi_{mn}^{\pm} = \exp\left(\pm i\int_m^n \xi(s)\mathrm{d}s\right)$ and the product of these functions. Using a cumulant expansion (in Gaussian Processes), we obtain

$$\langle\exp[\mathrm{ikx(t)}]\rangle = \exp\left[\mathrm{ik}\langle\langle \mathrm{x}(\mathrm{t}_1)\rangle\rangle + \frac{\mathrm{i}^2\mathrm{k}^2}{2!}\langle\langle \mathrm{x}(\mathrm{t}_1)\mathrm{x}(\mathrm{t}_2)\rangle\rangle + \ldots + \frac{\mathrm{i}^n\mathrm{k}^n}{\mathrm{n}!}\langle\langle \mathrm{x}(\mathrm{t}_1)\ldots\mathrm{x}(\mathrm{t}_n)\rangle\rangle\right] \tag{71}$$

where $\langle\langle x(t_1)...x(t_n)\rangle\rangle$ is referred to the cumulant of n-order. Finally, this is obtained:

$$\langle\rho_{\mathrm{ba}}^{(3)}(t)\rangle = \frac{2i\Omega_2{}^2\Omega_2^*\rho_{\mathrm{D}}^{(0)}\exp(ik_3 r)\exp(-i\omega_3 t)}{\left[\frac{1}{T_2^{\mathrm{eff}}} + i(\omega_0 - \omega_1)\right]\left[\frac{1}{T_1} - i(\omega_1 - \omega_2)\right]\left[\frac{1}{T_2^{\mathrm{eff}}} + i(\omega_0 - \omega_3)\right]}$$
$$+\frac{2i\Omega_2{}^2\Omega_2^*\rho_{\mathrm{D}}^{(0)}\exp(ik_3 r)\exp(-i\omega_3 t)}{\left[\frac{1}{T_2} - i(\omega_0 - \omega_2)\right]\left[\frac{1}{T_1} - i(\omega_1 - \omega_2)\right]\left[\frac{1}{T_2} + i(\omega_0 - \omega_3)\right]} \tag{72}$$

Here, we have defined: $1/T_2^{\mathrm{eff}} = 1/T_2 + 2\gamma$, where γ is the noise strength. Eq 72 is a central result of our analysis, whose scope reproduces proposals formulated by Yajima,[37] where the thermal reservoir (in our case the chemical solvent) can be observed as a homogeneous broadening of the resonance frequencies. Considering these matrix density elements for the coherences already averaged in the statistical ensemble, it is possible to obtain the corresponding macroscopic polarization of the form: $P^{\xi(3)}(\omega_3) = N\langle\langle\rho_{\mathrm{ba}}^{(3)}(\omega_3)\rangle_{\sigma}\mu_{\mathrm{ab}}\rangle_{\theta}$, or considering both the steady-state and the scalar approximations, we obtain

$$P^{\xi(3)}(\omega_3) = \chi^{\mathrm{solvent}}(\omega_3)E(\omega_3) + \chi_{\mathrm{eff}}^{\mathrm{coup}}(\omega_3)E_1{}^2E_2^* \tag{73}$$

In this case, the susceptibility is given by

$$\chi_{\mathrm{eff}}^{\mathrm{coup}}(\omega_3) = \frac{2iN\rho_{\mathrm{D}}^{(0)}\mu_{\mathrm{ba}}^4}{\hbar^3}\left\{\frac{1}{\left[\frac{1}{T_2^{\mathrm{eff}}} + i\Delta_1\right]}\frac{1}{\left[\frac{1}{T_1} - i\Delta\right]}\frac{1}{\left[\frac{1}{T_2^{\mathrm{eff}}} + i\Delta_3\right]}\right.$$
$$\left.+\frac{1}{\left[\frac{1}{T_2} - i\Delta_2^*\right]}\frac{1}{\left[\frac{1}{T_1} - i\Delta\right]}\frac{1}{\left[\frac{1}{T_2} + i\Delta_3\right]}\right\}$$

with $\Delta_j = \omega_0 - \omega_j$, $j = 1, 2, 3$. In Figure 11a and 11b is represented the absorption coefficient ($\propto Im\chi^{\mathrm{coup}}(\omega_3)$) and refractive index ($\propto Re\chi^{\mathrm{coup}}(\omega_3)$), respectively, as a function of the detuning (Δ_1, Δ_2), for the cases where the solvent does not influence the Bohr frequency shift, using MCG organic dye, with $\mu_{\mathrm{ba}} = 2.81 \times 10^{18}$ erg$^{1/2}$ cm$^{3/2}$ and $\omega_0 = 3.06 \times 10^{15}$ s^{-1}. Next, we observe how the surfaces derived from the absorption process and the scattering process show high symmetry as a function of the pumping beam detuning for test detuning values strictly equal to zero. In Figure 11a and 11b for the absorption coefficient and refractive index, respectively, as a function of the corresponding pump and probe detuning's, in the cases where the solvent is not treated as a stochastic type of process with no Bohr frequency shift, there is crossing characteristic of vibronic coupling, and the system is only represented as two levels with no details in its internal

https://doi.org/10.1021/acsomega.2c07300
ACS Omega 2023, 8, 10690−10712

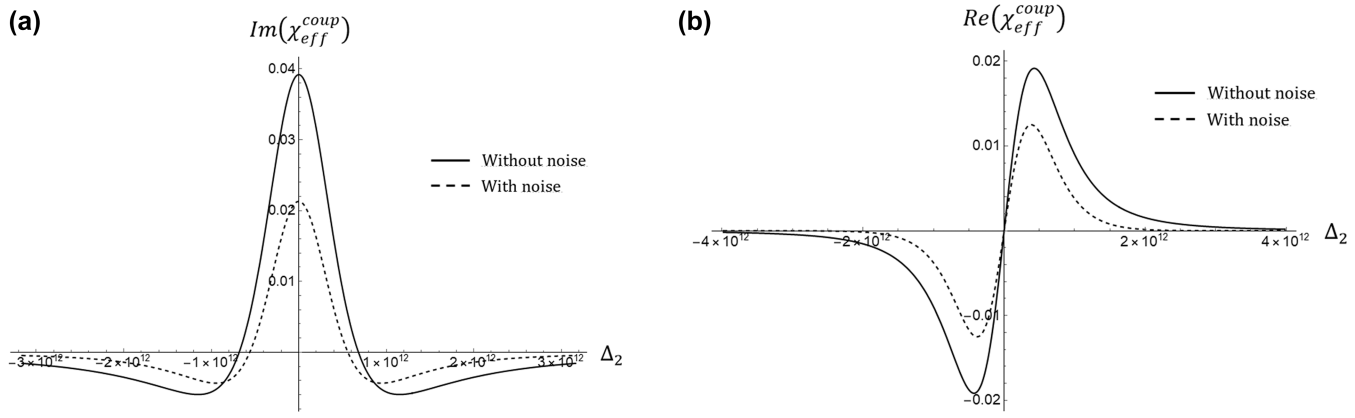

Figure 12. (a) Imaginary part and (b) real part of the susceptibility as a function of detuning Δ_2. Comparison of the optical responses in the presence and absence of both intramolecular coupling effects and noise caused by the solvent.

structure nature. It is important to highlight the fact that is presented in this Figure 11. We note in Figure 11a that for null tuning values in the test presents a maximum absorptive intensity when changing the detuning in the pumping beam. There is in this case a close symmetry of the response. However, when detuning is done in the pumping beam and running with the test beam, this symmetry appears to be broken. It is possible to examine this condition from the formulated expressions.

In Figure 11b, we observe that the dispersive property when varying with respect to Δ_1 at values of $\Delta_2 = 0$, the symmetry in the diffractive optical response is observed with a maximum of 0.5 and with a minimum of −0.5. It is important to note that as we move away from $\Delta_1 = \Delta_2 = 0$, however, the contrast decreases. We can conclude that in the cases of no solvent effect and described as a two-state system without vibronic coupling, the absorbing and scattering surfaces maintain high symmetry with respect to the pumping detuning for the zero value of the probe detuning. It is important to note that the chosen representations for both optical properties allow the simulation of a wide set of experiments, due to the difficulties inherent to the type of experiments in FWM spectroscopy, the simultaneous variation of pump and probe frequencies is very complicated. Finally, it is necessary to emphasize that our model focuses on the calculation of adiabatic coherences under stochastic solvent considerations. If in this development, we do not explicitly consider intramolecular effects, and our solute−solvent random interaction effect that shifts the Bohr frequency is associated with an inhomogeneous distribution of resonance frequencies, our result is the same as the one proposed by Yajima[37] that he was later able to experimentally verify by employing organic dyes when calculating optical susceptibilities.

2.4.2. Nonlinear Optical Properties: Simultaneous Effects of Intramolecular Coupling and Stochasticity of the Solvent. Herein, we examine for the nonlinear optical properties the behavior of their profiles subject to a simultaneity in both the solvent effect through the transition frequency shift and the details in their molecular structure. For the latter, we incorporate the residual spin−orbit Hamiltonian, generating a state crossover, and modifying the calculation basis in the coupled case to a decoupled one, thus allowing reformulations of the permanent and transition dipoles. This fact is mainly due to the reformulations in the energies and wave functions of the new calculation bases. Considering the expressions eqs 50a, 50b, and eqs 52−53 that define the energies as the permanent and transition dipole moments derived in the intramolecular coupling and considering the effects of the thermal reservoir for the transition between state |A⟩ and |B⟩, it is possible to generate the expression of the induced coherence, given by

$$\langle \rho_{BA}^{\xi(3)} \rangle_{\xi} = \frac{2i\Omega_1{}^2\Omega_2^{*}\tilde{\rho}_D^{(0)}\exp(ik_3 r)\exp(-i\omega_3 t)}{L_\Delta}\left(\frac{1}{L_1^{e}L_3^{e}} + \frac{1}{\tilde{L}_2\tilde{L}_3}\right) \tag{74}$$

where $L_j^{e} = \frac{1}{T_2^{e}} + i(\tilde{\omega}_0 - \omega_j)$, with $j = 1, 2$; $\tilde{L}_k = \frac{1}{\tilde{T}_2} + i(\tilde{\omega}_0 - \omega_k)$ with $k = 2,3$; $L_\Delta = \frac{1}{T_1} + i(\omega_1 - \omega_2)$, and where have derived an effective transversal relaxation time, defined as $\frac{1}{T_2^{e}} = \frac{1}{\tilde{T}_2} + 2\gamma$, where $\tilde{T}_2$ refers to the intramolecular coupling. It is important to note that because of the simultaneity in both effects, it is possible to derive an effective relaxation time, described additively in the relaxation processes due to solvent effects through the Bohr frequency shift associated with the intensity of the noise and the vibronic coupling as a manifestation of the details in the internal structure. Here, we have used the $\langle \xi \rangle_\sigma = \tilde{\omega}_0$ according to the central limit theorem.[65] Considering that the coupling susceptibility is a complex number, we can express its real and imaginary components as follows:

$$Im\chi_{eff}^{coup}(\Delta_1, \Delta_2) = A(\tilde{\omega}_0, \gamma)\left(f_{00} + \sum_{k+j=2} f_{kj}\Delta_1^k\Delta_2^j\right) \tag{75}$$

$$Re\chi_{eff}^{coup}(\Delta_1, \Delta_2) = A(\tilde{\omega}_0, \gamma)\left(\sum_{1\le k+j\le 3} g_{kj}\Delta_1^k\Delta_2^j\right) \tag{76}$$

$A(\tilde{\omega}_0, \gamma) = \frac{2N|\mu_{BA}|^4\tilde{\rho}_D^{(0)}}{\hbar^3 L_T}$; $f_{nm} = C_{n+2m+1}|\tilde{L}_2|^2|\tilde{L}_3|^2 + D_{n+2m+1}|L_1^{e}|^2|L_3^{e}|^2$; $g_{nm} = G_{n+2m+1}|\tilde{L}_2|^2|\tilde{L}_3|^2 - H_{n+2m+1}|L_1^{e}|^2|L_3^{e}|^2$, and where the coefficients are given by $C_1 = \frac{1}{T_1(T_2^{e})^2}$; $C_2 = \frac{2}{T_1} - \frac{3}{T_2^{e}}$; $C_3 = -\frac{1}{T_2^{e}}$; $C_4 = \frac{4}{T_2^{e}} + \frac{1}{T_1}$; $D_1 = \frac{1}{T_1(\tilde{T}_2)^2}$; $D_2 = -\frac{1}{\tilde{T}_2}$; $D_3 = -\left(\frac{1}{T_1} + \frac{2}{\tilde{T}_2}\right)$; $D_4 = \frac{2}{T_1} + \frac{4}{\tilde{T}_2}$; $G_1 = 2$; $G_2 = -\frac{3}{T_1T_2^{e}} - \frac{1}{(T_2^{e})^2}$; $G_3 = -\frac{2}{T_1T_2^{e}}$; $G_4 = -3$; $G_5 = -1$; $H_1 = 1$; $H_2 = \frac{1}{\tilde{T}_2}\left(\frac{2}{T_1} + \frac{1}{\tilde{T}_2}\right)$; $H_3 = -\frac{1}{\tilde{T}_2}\left(\frac{2}{T_1} + \frac{1}{\tilde{T}_2}\right)$; $H_4 = 2$; $H_5 = -3$. Here, we have defined: $L_T = (|L_1^{e}||L_3^{e}||\tilde{L}_2||\tilde{L}_3|$

https://doi.org/10.1021/acsomega.2c07300
ACS Omega 2023, 8, 10690−10712

$L_\Delta|)^2$. To account for the behavior of the optical responses when both effects are considered simultaneously, we present Figure 12, where we plot the imaginary and real components of the coupling susceptibility as a function of the frequency detuning of the probe-beam, when comparing in the presence and absence of the structure effects (intramolecular coupling) and of the solvent effect in terms of the random transition. We can observe that in both optical responses the intensity decreases strongly when considering the simultaneity of the effects. In trying to elucidate a valid reason that in the nonlinear optical properties their intensity decreases because of the incorporation of the intramolecular effect through the Hamiltonian recognizing the reason for the intensity decreases in the optical properties, it seems difficult to decipher the effect of the induction of vibronic coupling with the incorporation of residual spin−orbit Hamiltonians. However, in the case of solvent effects, caused by a shift of the Bohr frequency of the active system, which causes a broadening in the upper level and absorption are weakened. This total noise manifests itself through the transverse relaxation time, causing the susceptibility intensity to decrease in both its real and imaginary representation. This trend appears to be independent of whether the noise causes the time it takes for the system to lose coherence between the induced dipole moments to increase or decrease.

From our model for the optical properties, it is possible to derive important symmetry properties inherent to their behavior in the frequency space Δ_1, Δ_2. For cases where the refractive index $\eta^{(3)}(\omega_3) \approx \eta_0 = 1{,}333$ is similar in magnitude to the index of water, it is possible to redefine the absorption coefficient and express it as follows:

$$\tilde{\alpha}^{(3)}_{\Delta_1,\Delta_2} = \sum_{k+j=2} f_{kj}\Delta_1^2\Delta_2^2 \tag{77}$$

In view of the quadratic form of $\tilde{\alpha}^{(3)}_{\bar{\Delta}_1,\bar{\Delta}_2}$, it is possible to perform canonical transformations and express in function of its principal axes of symmetry and reach a form of the type:

$$\frac{\bar{\Delta}_1^2}{a^2} + \frac{\bar{\Delta}_2^2}{b^2} = 1 \text{ for } b^2 = \tilde{\alpha}^{(3)}_{\Delta_1,\Delta_2}/\lambda_2 \tag{78}$$

Here $\tilde{\alpha}^{(3)}_{\bar{\Delta}_1,\bar{\Delta}_2} = \lambda_1\bar{\Delta}_1^2 + \lambda_2\bar{\Delta}_2^2$, with $\lambda_1 = (f_{20} + f_{02} + \tilde{f})/2$, $\lambda_2 = (f_{20} + f_{02} - \tilde{f})/2$, $\tilde{f} = [(f_{20} - f_{02})^2 + f_{11}{}^2]^{1/2}$. This representation in the principal axes allows, through the evaluation of the axial and equatorial axes, the determination of relaxation times of interest in the characterization of the molecular system under study. The elliptic representations can provide insight for the study of the dissipation processes taking place in the transformed frequency space.

3. FINAL COMMENTS

The present review paper explores a detailed analysis of different theoretical models that allow the characterization of molecular systems through nonlinear optical responses. For this, we consider mainly the MCG organic dye, and we identify in it the longitudinal and transversal relaxation times, as well as the dipole moments and their transition frequency. All the studies performed refer to nonlinear FWM spectroscopy, both in degenerate and nondegenerate situations. The Liouville-Von Newman equation is used as a basis to identify the density matrix of the mixed states. The radiation−matter interaction is tested in all models under the electric-dipole approximation. The different models concern both perturbative regimes for the treatments of the light beams and those of saturative type for the pump-field. For the nature of photonic processes, we consider those of resonant character where the Rotating-Wave approximation is valid. The incorporated intramolecular coupling models allow the study of the optical responses subject to the change of basis and the insertion of residual Hamiltonians, the critical quantities of analysis being the permanent and transition dipole moments of the systems under study. The presence of the solvent under stochastic methodologies is characterized by the shift of the Bohr frequency to a time-dependent function. We estimate that solute−solvent collisions modify the Harmonic potential minima -preferentially vertically, since it is subject to a fixed nuclear coordinate broadening the upper-level of the transition. Our stochastic processes are governed by the Markovian approximation. We find that a description of the optical responses is best carried out in a coordinate space constituted by the frequency detuning's of pump- and probe-beams, as well as the intramolecular noise parameters and the stochastic process parameters. We noticed high sensitivity of the optical responses in relation to these study parameters, highlighting decreases the absorption or contrast of the refractive process in the presence of these processes. It is important to note that in FWM signals, tunable parametric amplification is possible with organic dyes, subject to the insertion of beams propagation effects in an optical length region. Derivations of noise-dependent effective transversal relaxation times simultaneously characterize both vibronic and stochastic processes. In relation to the different approaches used, as well as the considerations in the proposed model, we can estimate that our proposal is limited to certain materials with oriented dipole moments, for example, in those molecules that respond to solid matrices that can be associated with the solvent in a chemical solution. Our proposal is experimentally useful for the study of two-photon absorption processes, usually studied under explicit considerations of nonzero permanent dipole moments and considering antiresonance terms. Our model can be applied to molecules exhibiting Jahn−Teller type effects or in the cases of dimer excited states. The restrictive form can hopefully be fulfilled for quasi-degenerate vibrational states in the so-called weak intramolecular coupling. We propose that our studies through the developed model can be generalized to describe a variety of phenomena in both nanophotonic and plasmonic systems. Our results show the possibility of being used in the design and construction of optoelectronic devices that link with the use of optical sensors through the properties of the refractive index, as well as taking advantage of the properties of organic dyes and linking their properties with possible parametric amplifications derived from the propagation of fields in restricted optical lengths.

AUTHOR INFORMATION

Corresponding Author

José Luis Paz − *Departamento Académico de Química Inorgánica, Facultad de Química e Ingeniería Química, Universidad Nacional Mayor de San Marcos, Lima 15081, Perú;* orcid.org/0000-0002-6177-7919; Email: jpazr@unmsm.edu.pe

Authors

Marcos A. Loroño − *Departamento Académico de Fisicoquímica, Facultad de Química e Ingeniería Química, Universidad Nacional Mayor de San Marcos, Lima 15081, Perú*

https://doi.org/10.1021/acsomega.2c07300
ACS Omega 2023, 8, 10690−10712

Lenin A. González-Paz − *Centro de Biomedicina Molecular (CBM). Laboratorio de Biocomputación (LB), Instituto Venezolano de Investigaciones Científicas (IVIC), 4001 Maracaibo, Zulia, República Bolivariana de Venezuela*

Edgar Márquez − *Grupo de Investigaciones en Química y Biología, Departamento de Química y Biología, Facultad de Ciencias Exactas, Universidad del Norte, Barranquilla 081007, Colombia*

José R. Mora − *Instituto de Simulación Computacional (ISC-USFQ), Departamento de Ingeniería Química, Universidad San Francisco de Quito (USFQ), Quito 170901, Ecuador;* orcid.org/0000-0001-6128-9504

Ysaias J. Alvarado − *Centro de Biomedicina Molecular (CBM), Laboratorio de Química Biofísica Teórica y Experimental (LQBTE), Instituto Venezolano de Investigaciones Científicas (IVIC), 4001 Maracaibo, Zulia, República Bolivariana de Venezuela;* orcid.org/0000-0002-2709-409X

Complete contact information is available at: https://pubs.acs.org/10.1021/acsomega.2c07300

Author Contributions

José Luis Paz: Conceptualization, Data curation, Formal analysis, investigation, Methodology, Writing-original draft; **Marcos A. Loroño:** Supervision, Validation, Writing-original draft; **Lenin-González−Paz:** Supervision, Writing-review & editing; **Edgar Márquez:** Supervision, Validation, Writing-original draft; **José Ramón Mora:** Supervision, Validation, Writing-original draft; **Ysaias Alvarado:** Conceptualization, Data curation, Formal analysis, investigation, Methodology, Writing-original draft.

Notes

The authors declare no competing financial interest.

■ ACKNOWLEDGMENTS

The work was carried out using the computational resources provided by the Universidad Nacional Mayor de San Marcos through its Vice Rectorate of Research and Postgraduate Studies. The authors express their deep gratitude to all the reviewers of this study for their critical reading and recommendations that guaranteed an increase in the quality of the manuscript.

■ REFERENCES

(1) Boyd, R. W. *Nonlinear Optics*; Academic Press: New York, 2008.

(2) Colmenares, P. J.; Almeida, R.; Paz, J. L. Stochastic effects of the solvent on the absorptive and dispersive processes in a two-level system up to first order in the external field. *J. Phys. B: At. Mol. Opt. Phys.* **1995**, *28*, 4377−4388.

(3) García-Golding, F.; Marcano O., A. High-order effects in Rayleigh-type optical mixing. *Phys. Rev. A* **1985**, *32*, 1526−1530.

(4) Song, J. J.; Lee, J. H.; Levenson, M. D. Picosecond relaxation measurements by polarization spectroscopy in condensed phases. *Phys. Rev. A* **1978**, *17*, 1439−1447.

(5) García-Golding, F. Spectral diffusion effects in polarization spectroscopy. *J. Opt. Soc. Am. B* **1983**, *73*, 59−62.

(6) Mourou, G. Spectral hole burning in Dye solutions. *IEEE J. Quantum Electron.* **1975**, *11*, 1−8.

(7) Lee, J. H.; Song, J. J.; Scarparo, M. A. F.; Levenson, M. D. Coherent population oscillations and hole burning observed in Sm^{+2}: CaF_2 using polarization spectroscopy. *Opt. Lett.* **1980**, *5*, 196−198.

(8) Yajima, T.; Souma, H.; Ishida, Y. Study of ultrafast relaxation processes by resonant Rayleigh-type optical mixing II. Experiments on dye solutions. *Phys. Rev. A* **1978**, *17*, 324−334.

(9) Souma, H.; Yajima, T.; Taira, Y. Ultrafast relaxation study by resonant Rayleigh-type optical mixing spectroscopy using picosecond light pulses. *J. Phys. Soc. Jpn.* **1980**, *48*, 2040−2047.

(10) Yang, Y.; He, J.; Zhang, W.; Xiao, H.; Liu, J. A novel chromophore containing a Michler's donor and a tricyanofuran acceptor with enhanced nonlinear optical properties. *Mater. Lett.* **2019**, *255*, 126555.

(11) Edet, C.O.; Al, E.B.; Ungan, F.; Ali, N.; Ramli, M.M.; Asjad, M. Effects of the confinement potential parameters and optical intensity on the linear and nonlinear optical properties of spherical quantum dots. *Results Phys.* **2023**, *44*, 106182.

(12) Durak, S.; Sakiroglu, S. Theoretical investigation of laser field effect on nonlinear optical properties of quantum dots. *Physica B* **2023**, *650*, 414575.

(13) Yaqub, N.; Farooq, W.A.; AlSalhi, M.S. Nonlinear optical properties of LLDPE composites with titanium dioxide anatase phase. *J. King Saud Univ. Sci.* **2022**, *34*, 101723.

(14) Zhang, Q.; Bai, Q.; Cai, E.; Hao, L.; Wang, M.; Zhang, S.; Zhao, Q.; Teng, L.; Sui, N.; Du, F.; Wang, X. Nonlinear optical properties of graphdiyne/graphene van der Waals heterostructure for laser modulations. *Results Phys.* **2022**, *38*, 105654.

(15) Fouejio, D.; Tadjouteu Assatse, Y.; Yossa Kamsi, R. A.; Ejuh, G. W.; Ndjaka, J. M. B. Structural, electronic and nonlinear optical properties, reactivity and solubility of the drug dihydroartemisinin functionalized on the carbon nanotube. *Heliyon* **2023**, *9*, No. e12663.

(16) Fan, W.; He, J.; Wei, H.; Zhang, C.; Zhu, M.; Xu, D.; Xiao, A.; et al. Broadband nonlinear optical properties of red fluorescent carbon dots. *Results Phys.* **2022**, *38*, 105591.

(17) Al-Saidi, I.A.-D.H.A.; Abdulkareem, S.A.-D. Nonlinear optical properties and optical power limiting effect of Giemsa dye. *Opt. Laser. Technol.* **2016**, *82*, 150−156.

(18) Weisman, P.; Wilson-Gordon, A. D.; Friedmann, H. Effect of propagation on pulsed four-wave mixing. *Phys. Rev. A* **2000**, *61*, 053816.

(19) Cao, W. Improved compensation of intrachannel four-wave mixing in dispersion-managed transmission links with mid-span optical phase conjugation. *Opt. Commun.* **2023**, *530*, 129185.

(20) Wang, Y.; Yang, L.; Zhang, L.; Dai, S. Compact Brillouin comb laser in Chalcogenide fiber assisted by four-wave mixing. *Infrared Phys. Technol.* **2022**, *127*, 104431.

(21) Rehman, H. U.; Awan, A. U.; Abro, K. A.; Tag El Din, E. M.; Jafar, S.; Galal, A. M. A non-linear study of optical solitons for Kaup-Newell equation without four-wave mixing. *J. King Saud Univ. Sci.* **2022**, *34*, 102056.

(22) Nguyen, T. T.; Tsai, C. C. Four-wave mixing involving Ξ-*V* type system: In view of dressed state picture. *Chin. J. Phys.* **2022**, *77*, 319−326.

(23) Wang, X.; Yuan, J.; Wang, L.; Xiao, L.; Jia, S. Enhanced frequency up-conversion based on four-wave mixing assisted by a Bessel-Gaussian beam in ^{85}Rb atoms. *Opt. Laser Technol.* **2022**, *149*, 107874.

(24) Ahmad, H.; Kamely, A. A.; Zaini, M. K. A.; Samion, M. Z.; Chong, W. Y.; Zamzuri, A. K.; Lim, K. S. Generation of four-wave mixing with nonlinear Vanadium-carbide (V_2C)-deposited side-polished fiber (SPF) in 1.5- and 2.0-μm wavelength operation. *Opt. Laser Technol.* **2022**, *145*, 107458.

(25) Dong, A.; Zhang, K.; Jing, J. Generation of twelve-partite entanglement from two symmetric four-wave mixing processes. *Opt. Commun.* **2022**, *521*, 128470.

(26) De, A. K.; Goswami, D. Towards controlling molecular motions in fluorescence microscopy and optical trapping a spatiotemporal approach. *Int. Rev. Phys. Chem.* **2011**, *30*, 275−299.

(27) Goswami, D. Optical pulse shaping approaches to coherent control. *Phys. Rep.* **2003**, *374*, 385−481.

(28) Diniz, K.; Dutra, R. S.; Pires, L. B.; Viana, N. B.; Nussenzveig, H. M.; Maia-Neto, P. A. Negative optical torque on a microsphere in optical tweezers. *Opt. Express* **2019**, *27*, 5905−5917.

(29) Abozied, A. M.; Mostafa, A. M.; Abouelsayed, A.; Hassan, A. F.; Ramadan, A. A.; Al-Ashkar, E. A.; Anis, B. Preparation, characterization, and nonlinear optical properties of graphene oxide thin film doped with

low chirality metallic SWCNTs. *J. Mater. Res. Technol.* **2021**, *12*, 1461−1472.
(30) Zeiri, N.; Naifar, A.; Abdi-Ben Nasrallah, S.; Said, M. Dielectric environment effect on linear and nonlinear optical properties for CdS/ZnS core/shell quantum dots. *Results Phys.* **2019**, *15*, 102661.
(31) Onyenegecha, C. P. Linear and nonlinear optical properties in spherical quantum dots: Modified Möbius squared potential. *Heliyon* **2022**, *8*, No. e10387.
(32) Noudem, P.; Fouejio, D.; Mveme, C. D. D.; Zekeng, S. S.; Fankam Fankam, J. B. Impact of doping on the optoelectronic, electronic, and nonlinear optical properties and on the reactivity of photochromic polymers containing styrylquinoline fragments: Hartree-Fock and DFT study. *Heliyon* **2022**, *8*, No. e11491.
(33) Apanasevich, P. A.; Kilin, S. Ya.; Nizovtsev, A. P.; Onishchenko, N. S. Оп anomalouš Free induction decay rate. *Opt. Commun.* **1984**, *52*, 279−282.
(34) Berman, P. R. Brownian motion of atomic systems: Fokker-Planck limit of the transport equation. *Phys. Rev. A* **1974**, *9*, 2170−2177.
(35) Colmenares, P. J.; Paz, J. L. 2011 On the analytical solution of the Optical Bloch equation. *Opt. Commun.* **2011**, *284*, 5171−5176.
(36) Toutounji, M. A deeper look into Herzberg-Teller vibronic coupling effect and spectroscopy signature of non-Condon systems. *Chem. Phys.* **2019**, *523*, 205−210.
(37) Yajima, T. Non-linear optical spectroscopy of an inhomogeneously broadened resonant transition by means of three-wave mixing. *Opt. Commun.* **1975**, *14*, 378−382.
(38) Blum, K. *Density Matrix Theory and Applications*; Plenum: New York, 1981.
(39) Mollow, B. R. Propagation of Intense Coherent Light Waves in Resonant Media. *Phys. Rev. A* **1973**, *7*, 1319−1321.
(40) Boyd, R. W.; Raymer, M. G.; Narum, P.; Harter, D. J. Four-wave parametric interactions in a strongly driven two-level system. *Phys. Rev. A* **1981**, *24*, 411−423.
(41) Agarwal, G. S.; Nayak, N. Multiphoton processes in two-level atoms in two intense pump beams. *J. Opt. Soc. Am. B* **1984**, *1*, 164−168.
(42) Agarwal, G. S.; Nayak, N. Effects of collisions and saturation on multiphoton processes and nonlinear mixing in the field of two pumps. *Phys. Rev. A* **1986**, *33*, 391−402.
(43) Paz, J. L.; Gorayeb, M.; Hernández, A. J. Optical properties in a two-level system: Stochastic Considerations. *J. Mol. Struct. (THEOCHEM)* **2006**, *769*, 19−26.
(44) Boyd, R. W.; Sargent, M. Population pulsations and the dynamic Stark effect. *J. Opt. Soc. Am. B* **1988**, *5*, 99111.
(45) Gruneisen, M. T.; MacDonald, K. R.; Boyd, R. W. Induced gain and modified absorption of a weak probe beam in a strongly driven sodium vapor. *J. Opt. Soc. Am. B* **1988**, *5*, 123−129.
(46) Paz, J. L.; Franco, H. J.; Reif, I.; Marcano O., A.; García-Golding, F. Pump-power dependence due to parametric amplification of the Rayleigh-type optical-mixing signal. *Phys. Rev. A* **1988**, *37*, 3381−3385.
(47) Franco, H. J.; Paz, J. L.; Marcano O., A.; Salazar, M. C.; Reif, I. Symmetry properties of the Rayleigh-type optical mixing signal in frequency space. *J. Opt. Soc. Am. B* **1990**, *7*, 57−63.
(48) Reif, I.; García-Golding, F.; Paz, J. L.; Franco, H. J. Three-levels of approximation in the study of the propagation of the Rayleigh-type optical mixing signal. *J. Opt. Soc. Am. B* **1991**, *8*, 2470−2476.
(49) Márquez, L.; Reif, I.; Franco, H. J.; Marcano O., A.; Paz, J. L. High-pump power effects on resonant nearly degenerate four-wave mixing signal for homogeneously and inhomogeneously broadened two-level systems. *Phys. Rev. A* **1993**, *47*, 4185−4192.
(50) Paz, J. L.; Cardenas, A. E.; Hernandez, A. J.; Franco, H. J. effects of the spectral inhomogeneity on the approximation levels for the study of the propagation of the Rayleigh-type optical mixing signal. *Opt. Commun.* **1994**, *109*, 195−204.
(51) Paz, J. L.; Bessega, C.; Cardenas, A. E.; Hernández, A. J. Study characterization of new resonances in the frequency space in a two-level system with nonzero permanent dipole moments. *J. of Phys. B: At. Mol. Phys. Opt.* **1995**, *28*, 5377−5395.
(52) Islam, S.; Abdullah, M. Structural and 3rd order nonlinear optical properties of organic dyes immobilized silica nanocomposite. *Opt. Mater.* **2020**, *106*, 110034.
(53) Lamaignere, L.; Toci, G.; Patrizi, B.; Vannini, M.; Pirri, A.; Fanetti, S.; Bini, R.; Mennerat, G.; Melninkaitis, A.; Lukas, L.; Hein, J. Determination of non-linear refractive index of laser crystals and ceramics via different optical techniques. *Opt. Mater: X* **2020**, *8*, 100065.
(54) Moncada, F.; Paz, J. L.; Lascano, L.; Costa-Vera, C. Effects of spectral diffusion on the nonlinear optical properties in two- and three-state quantum systems in a four-wave mixing signal. *J. Nonlinear Opt. Phys. Matter.* **2018**, *27*, 1850038.
(55) Dunn, J. L.; Alqannas, H. S.; Lakin, A. J. Jahn-Teller effects, and Surface interactions in multiply charged fullerene anions and the effect on scanning tunneling microscopy images. *Chem. Phys.* **2015**, *460*, 14−25.
(56) Qian, Y.; Li, X.; Harutyunyan, A. R.; Chen, G.; Rao, Y.; Chen, H. Herzberg-Teller Effect on the Vibrationally Resolved Absorption Spectra of Single-Crystalline Pentacene at Finite temperatures. *J. Phys. Chem. A* **2020**, *124*, 9156−9165.
(57) Fulton, R.; Gouterman, M. Vibronic coupling II spectra of dimers. *J. Chem. Phys.* **1964**, *41*, 2280−2286.
(58) Bohm, A.; Nostafazadeh, A.; Koizumi, H.; Niu, Q.; Zwanziger, J. Crossing of potential energy surfaces and the molecular Aharonov Bohm effect. In *The Geometric Phase in Quantum Systems*; Springer: Berlin, 2003; pp 195−224. DOI: 10.1007/978-3-662-10333-3_9.
(59) Teller, E. The crossing of potential surfaces. *J. Phys. Chem.* **1937**, *41*, 109−116.
(60) Di Bartolo, B. *Radiationless Processes*; Springer: NY, 1980.
(61) Yang, S.; Zhang, Q.-Y.; Zhu, Z.-W.; Qi, Y.-Y.; Li, L.; Lin, X.-C. Self-parametric amplification of a bound-state dissipative soliton assisted by spectral filtering effect in the negative dispersion regime. *Chaos, Solitons Fractals* **2022**, *164*, 112733.
(62) Sreenath, M. C.; Joe, I. H.; Rastogi, V. K. Reverse saturable absorption behavior of Disodium 8-Hydroxy-5,7-Dinitro-2-Naphthalenesulfonate Hydrate for nonlinear optical applications. *J. Mol. Struct.* **2019**, *1180*, 363−377.
(63) Wodkiewicz, K. Stochastic incoherences of optical Bloch equations. *Phys. Rev. A* **1979**, *19*, 1686−1696.
(64) Colmenares, P. J.; Paz, J. L.; Almeida, R.; Squitieri, E. Simultaneous stochastic effects of a thermal reservoir and an electromagnetic field on the optical susceptibility of a two-level system. *J. Mol. Struct. (THEOCHEM)* **1997**, *390*, 33−38.
(65) Van Kampen, N. G. *Stochastic Processes in Physics*; North-Holland: New York, 1981.
(66) Sreenath, M.C.; Hubert Joe, I.; Rastogi, V.K. Effect of solvents on the nonlinear optical behavior and spectral findings of bis [4-(dimethylamino) phenyl] methaniminium chloride. *Chem. Phys. Lett.* **2020**, *738*, 136833.
(67) Paz, J. L.; Loroño, M.; González-Paz, L.; Márquez, E.; Vera-Villalobos, J.; Mora, J. R.; Alvarado, Y. J. Nonlinear optical responses of molecular systems with vibronic coupling in fluctuating environments. *J. Nonlinear Opt. Phys. Matter.* **2022**, *31*, 2150011.

https://doi.org/10.1021/acsomega.2c07300
ACS Omega 2023, 8, 10690−10712